Trans. Indian Inst. Met.
Vol.57, No. 6, December 2004, pp. 537-577

COMPLEXITIES IN FATIGUE OF ENGINEERING MATERIALS AT ELEVATED TEMPERATURES

K. Bhanu Sankara Rao
Mechanical Metallurgy Division
Indira Gandhi Centre for Atomic Research, Kalpakkam 603 102
e-mail: bhanu@igcar.ernet.in

(Received 22 November 2004 ; in revised form 10 January 2005)

PREAMBLE

I express my deep sense of gratitude to the Indian Institute of Metals for the great honour it has bestowed on me by conferring the G.D. Birla Gold Medal for the year 2004. It is a matter of pride to join the select band of very distinguished metallurgists of the country who have made outstanding research contributions to the field of Materials Science and Engineering. I feel extremely happy that my humble contributions in the field of materials science and engineering have been recognized by my peers by selecting me for the G.D. Birla Gold Medal Award.

My research work started at Bhabha Atomic Research Centre, Bombay in 1974 on the development of copper base alloys for resistance welding electrodes by employing casting and powder metallurgical routes as a part of my M.Tech course in physical metallurgy at IIT Bombay. I have continued my research interest in powder metallurgy during my tenure as a Lecturer at Regional Engineering College, Warangal during 1975-77. Subsequently I have moved to Mechanical Metallurgy Group at Reactor Research Centre (RRC) (now Indira Gandhi Centre for Atomic Research IGCAR) Kalpakkam. In retrospect I feel that this was the most significant and fortunate decision I took in my career. Work in the area of mechanical metallurgy at Kalpakkam was initiated and nurtured for over 25 years by Dr. Placid Rodriguez whose personal example of dedication to work and emphasis on meaningful novelty and research have been an inspiration and beacon light to guide the progress in my research career. He has provided the umbrella under which, work in many areas including mechanical metallurgy flourished at Kalpakkam. He has been my principal mentor and supervisor of my Ph.D. research work.

At Kalpakkam, I have been a member of a team that set up facilities for materials development and evaluation of mechanical properties. This gave me an opportunity to interact with Dr. S.L. Mannan who acted as a friend, philosopher and guide in the formative years of my research career. In all my endeavours at Kalpakkam he has remained as a valued co-researcher. I have developed a special interest in mechanical metallurgy as I could foresee the important contributions that are required in materials development and characterization of mechanical properties, for the development of Fast Breeder Reactor (FBR) Technology in India. We have established facilities for fatigue research at RRC during 1980 and to our surprise we found that there is a lack of consensus on several issues in low cycle fatigue and creep-fatigue interaction testing that has severely impaired the generation of meaningful data for the design of FBRs. We realized the need for standardization of testing methodology and undertook a serious campaign to assess the various factors responsible for intra and inter-laboratory variability in Low Cycle Fatigue (LCF) properties. In a short span of time we were able to provide a unified criterion for the determination of strain hardening exponent that serves as a guide in the selection of materials, crack initiation and failure life in laboratory specimens. These definitions have been universally accepted today. Subsequently we have laid a major emphasis on characterization of the effects of microstructure and various testing variables on phenomenological and micro mechanistic aspects on FBR structural materials including stainless steels,

ferritic steels, superalloys and their weldments. This enabled us to develop a deeper understanding of the various time and temperature dependent phenomena influencing the LCF properties and facilitated the selection of materials, appropriate life prediction techniques and fix limits to their extrapolation. The information generated has also been found useful in formulation of the constitutive equations and design rules for FBR materials and their weldments. We also have the distinction of discovering uniform matrix cavitation in high temperature fatigue, establishing various manifestations of dynamic strain ageing in fatigue and defining the procedures for determination of various time and temperature dependent processes and their synergistic interactions. Over the years I have been engaged in research activities pertaining to materials development, tensile deformation and fracture, creep, low cycle fatigue, creep-fatigue interaction, thermomechanical fatigue, structure-property correlations, life assessment and prediction. Deeper understanding of the above mentioned subjects necessitated extended discussions with various experts at IGCAR, Kalpakkam. I have benefited from the meaningful discussions that I had on the above subjects with Dr. Baldev Raj since the beginning of my research career. This in retrospect has proved to be a boon that we have entered into a new territory of research comprising of correlation between microstructure, mechanical properties and non-destructive testing parameters. In the last decade we were able to establish correlations between various NDT parameters and cyclic softening, hardening, fatigue crack initiation and propagation, creep deformation and fracture, development of substructure, precipitation of various phases and their growth in stainless steels, ferritic steels and superalloys. These studies have been found indispensable in structural integrity assessment and life assessment of the power plant components. Recently we were able to contribute an invited review paper on "Assessment of Microstructures and Mechanical Behaviour of Metallic Materials through Non-Destructive Characterization" to International Materials Reviews. Dr. Baldev Raj , Director, IGCAR, Kalpakkam who himself being a distinguished Scientist and metallurgist of high repute set stiff standards for all of us to emulate and provided stimulatory environment, encouragement and support. Mechanical Metallurgy Division at IGCAR, Kalpakkam today has been recognized both nationally and internationally for many original contributions in the area of high temperature deformation and fracture of materials required in support of the FBR programme.

I have been deputed to Kernforschungsanlage, Juelich, Germany under Indo-German Bilateral agreement in 1984 for a period of 16 months. This gave me an opportunity to work on time dependent fatigue and creep-fatigue interaction of high temperature gas cooled reactor materials under the able guidance of Dr. H. Schuster and Prof. H. Nickel. These studies have provided mechanistic understanding and much needed information on the design rules of heat exchanger components. In 1993, I have been awarded National Research Council of USA fellowship to work as a Guest Scientist and Resident Research Associate at NASA-Lewis Research Center, Cleveland for a period of two years. NASA-Lewis Research Center has been a world leader in high temperature fatigue since the discovery of Manson-Coffin relationship in 1954 and this fellowship provided me a unique opportunity to work on aerospace materials under the stewardship of Dr. G.R. Halford. My contributions at NASA-Lewis Research Center resulted in understanding of complexities in the fatigue behaviour of superalloys, intermetallics and fiber reinforced metal-matrix composites.

In my presentation of the G.D. Birla Gold Medal Lecture today, I will not be able to do justice to all the areas of my research work that culminated in the publication of more than 250 research papers. I have therefore chosen to review certain aspects of my work with emphasis on high temperature fatigue which resulted in advancement of knowledge base on several stainless steels and their weldments, superalloys, nickel aluminides and SiC continuous fiber reinforced metal matrix composite.

1. INTRODUCTION

Low cycle fatigue is an important consideration in the design and operation of high temperature systems that are subjected to repeated thermal stresses as a result of temperature gradients which occur on heating and cooling during start-up and shut-downs or during the thermal transients[1-3]. On-load periods at elevated temperatures introduce time-dependent effects, most

importantly creep among many other effects. The systems that can undergo thermal transients include nuclear pressure vessels, steam turbines, aircraft gas turbines, heat exchangers and fuel elements, automobile parts and power plant components etc. In order to represent the component behaviour in a laboratory test, the thermal strains are replaced by mechanical strain and controlled under isothermal conditions. The slow start-up and shut-down cycle is replaced by a symmerrtrical and a continuous cycle of equal strain rates in tension and compression (Fig. 1), with a hold period at a constant peak strain to simulate the on-load period, i.e., creep-fatigue interaction. Slow-fast and fast-slow strain-time waveforms represent another category used to evaluate creep fatigue interaction effects.

Thermal stresses within a component are often highly localized and deformation constrained by surrounding material and thus generally result in strain controlled deformations. LCF failures represent a predominant failure mode, necessitating significant consideration in the design and life analysis of aforementioned components. Towards the goal of developing an accurate and sufficiently general life analysis tool, it is essential that the incorporated material behaviour model be physically based, representing features associated with the dominant fatigue deformation and damage mechanisms. This ultimately requires a comprehensive understanding of both the macroscopic cyclic deformation behaviour under the appropriate loading conditions, and the micromechanisms which influence such behaviours, as revealed in the deformation substructure and failure modes. Further, this understanding must include not only the behaviour at the maximum operating temperatures, but also the behaviour at the lower temperatures encountered during transients. This is obiviously a challenging task, given that high temperature material behaviour is often a function of the synergestic interactions of various time and temperature dependent variables/ phenomena, such as slip mode, oxidation damage, creep damage, dynamic strain ageing, dynamic precipitation and phase instabilities, inelastic deformation, deformation ratchetting, mean stress[3-8], and many others. Depending on the type of alloy and the metallurgical condition of the material, the effects of these time-dependent processes on cyclic stress response may be considerable and, in the worst case may reduce cyclic life by orders of magnitude as compared to room temperature value. By studying the deformation substructure and damage behaviour as a function of temperature, it is possible to obtain deeper insight into various time-dependent processes, their interactions, and other factors deteriorating the fatigue life at elevated temperatures. Such studies are of immense importance for developing constitutive equations in different temperature regimes. The generation of such information would also facilitate the development and selection of appropriate predictive methods and fix limits to their extrapolation.

In addition to creep and fatigue loading, operating conditions in reactor vessels and aero engines involve thermal transients with mechanical strain cycles[9-11]. This thermomechanical fatigue (TMF) loading often governs the lifetime of many high-temperature components. However, TMF tests are seldom carried out for generating data pertaining to material selection and qualification, primarily on account of the huge experimental efforts involved and the large number of test parameters that must be set for TMF testing in contrast to the conventional isothermal fatigue testing. Consequently, isothermal LCF tests performed at the maximum temperature of the expected TMF loading cycle are generally used as a basis for TMF lifetime prediction. This procedure, however, could involve considerable uncertainties especially if the development of the cyclic stress-strain response and the evolution of microstructure and micromechanisms of crack initiation and propagation are different from those under isothermal conditions. Often, the type and rate of occurrence of time and temperature dependent damage mechanisms and their interactions leading to failure in TMF conditions may be different than under isothermal LCF conditions. Therefore, the evaluation of TMF behaviour of materials used in critical applications has become indispensable. In an effort to examine the phenomenological effects of various testing variables and characterize the micromechanisms active during high temperature loadings, detailed investigations have been performed over the years under isothermal, creep-fatigue and TMF loading conditions on materials of interest to FBRs, gas cooled reactors and aero engines. Some of the salient findings are presented in this paper.

2. EFFECTS OF MICROSTRUCTURE ON LOW CYCLE FATIGUE BEHAVIOUR

The cyclic deformation and fracture of austenitic stainless steels engineered for high temperature applications depend critically on the initial microstructure [grain size (GS), prior cold work (PCW) and thermal ageing (TA)] and slip mode, both of which in turn depending on temperature, govern the cyclic stress response and the mode of crack initiation and propagation. In FBRs, for the core components, cold worked austenitic stainless steels are often recommended to reduce radiation induced void swelling. During fabrication of the sheets and plates into vessels, tanks, pipings, heat exchangers, etc., cold work may be introduced unintentionally and its influence on elevated temperature behaviour is to be accounted in the design.

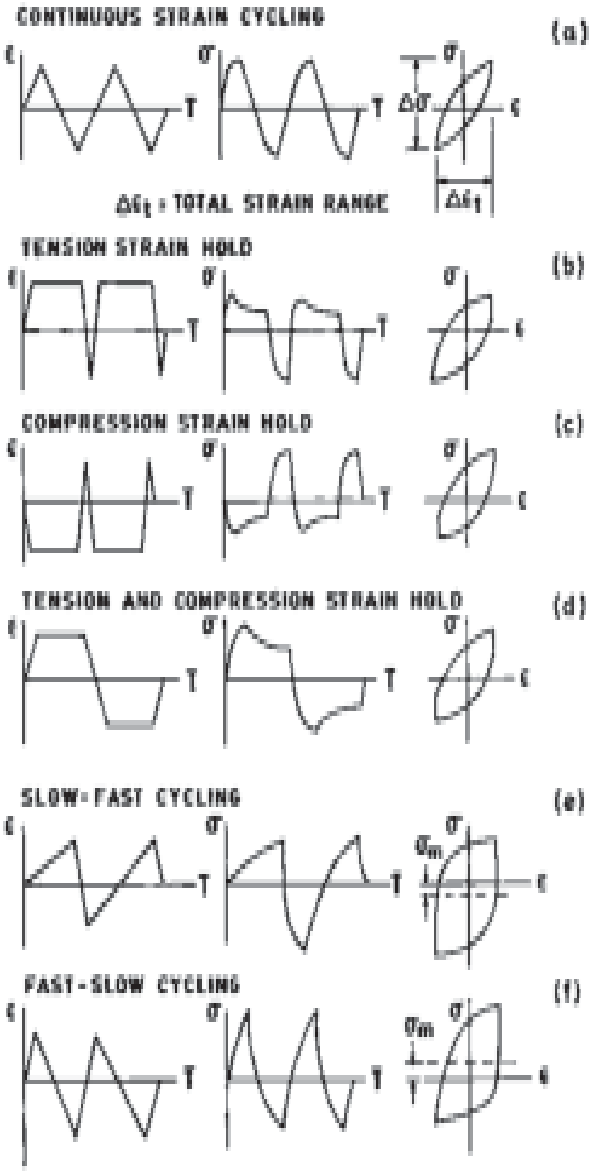

Fig. 1: Typical waveforms for strain controlled fatigue testing

2.1 Grain Size Effects on Strain Controlled LCF Behaviour of Type 304 Stainless Steel

The GS dependence of LCF life of a meta stable type 304 stainless steel in the range 300 to 1023 K has been investigated in detail[2,6,12,13]. LCF life was found to be strongly dependent on GS, temperature and strain amplitude employed in the testing (Figs. 2a & b). In general, fine GS exhibited better fatigue resistance, an exception to this being the results at 300 K at high strain amplitudes where increasing GS

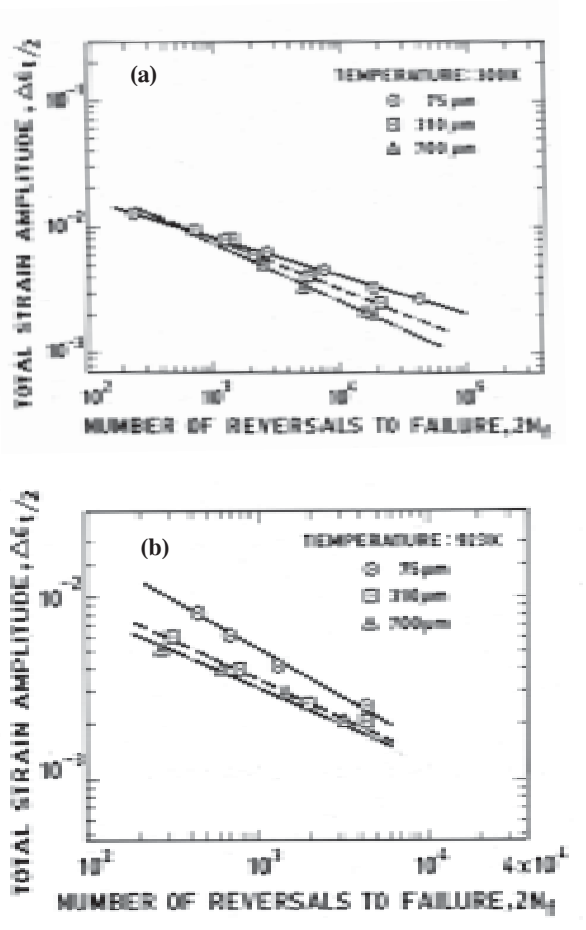

Fig. 2: Influence of grain size on LCF life at (a) 300 K and (b) 923 K[2]

showed a tendency for improved fatigue resistance. The improved life at 300 K in coarse GS at high strain amplitudes resulted from the beneficial effects arising from the deformation induced transformation of austenite to α'-martensite at the crack tip. Martensite formed around the crack tip absorbs the strain energy and suppress the crack propagation by producing residual compressive stresses[14,15]. No martensite could be found in fine GS material at the crack tip.

The beneficial effect of fine GS seems to result from both the extended crack initiation and propagation stages. Since the GS governs the slip length[16], a small grain size can be expected to develop smaller steps at the surface, which would render the formation of intrusions and extrusions more difficult. Because of the greater constraints to slip in finer GS material a large number of slip systems are required to operate, to generate the required strain. The constraint and corresponding reduction in slip per band make the crack initiation event a more difficult process in fine grained material than in coarse grained alloy. The improved crack propagation resistance with decreasing GS in alloys deforming by planar slip has been ascribed to the fact that grain boundaries act as the natural barriers for transgranular crack propagation[17] causing the crack front to be held back and necessitating the crack reinitiation event to occur in each new grain.

In all the grain sizes, life decreased drastically with increasing temperature upto 923 K (Fig. 3) The temperature effect on the reduction in life at elevated temperatures has generally been attributed to the increased inelastic strain in a given cycle, creep damage, and oxidation. The temperature dependence of inelastic strain in all the grain size showed a

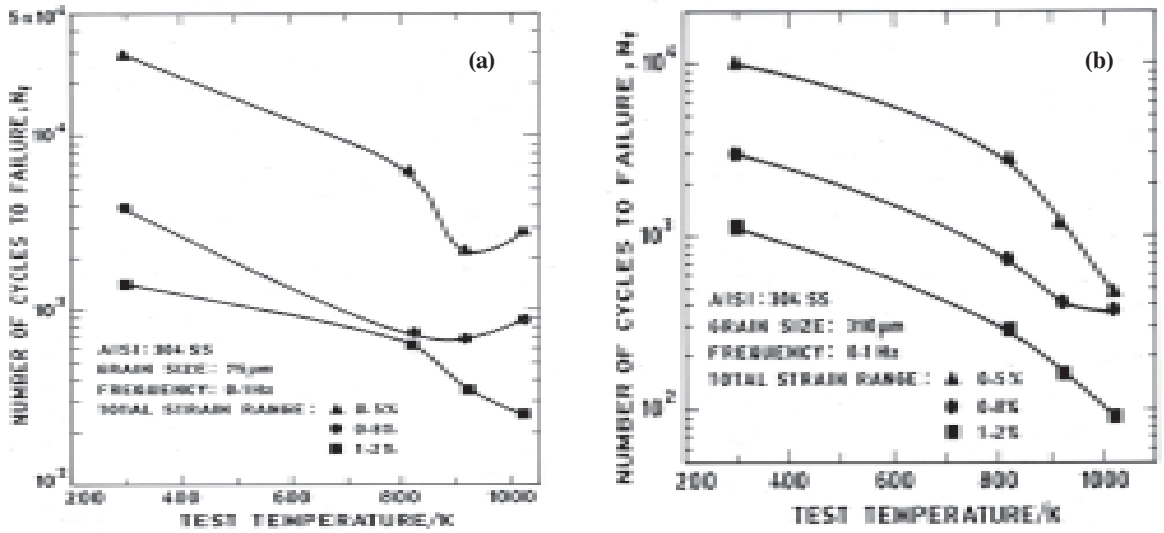

Fig. 3:Effect of temperature on fatigue life at different strain ranges for (a) fine grain and (b) medium Grain sized material.

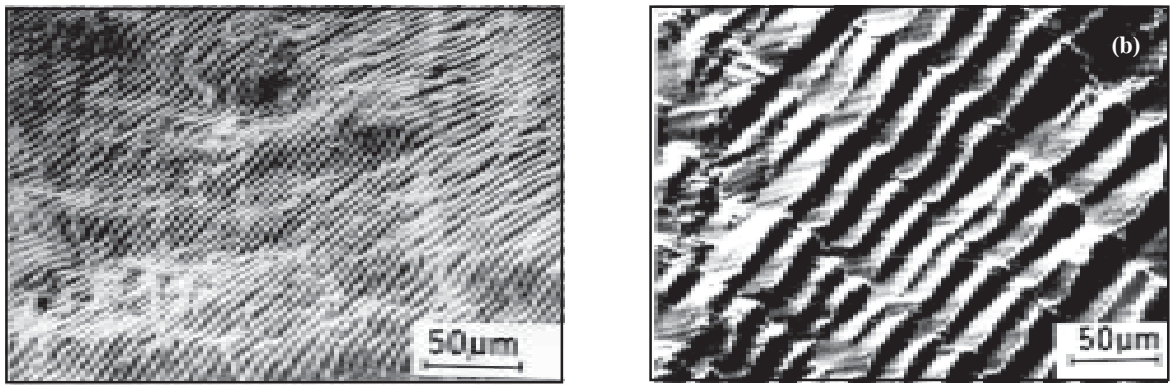

Fig. 4: (a) Ductile striations on the fracture surface of the sample tested at 300 K and (b) brittle striations at 823 K at a total strain amplitude of $+0.6\%$[2].

minimum at 823 K, and still a drastic reduction in life was observed due to DSA effects. The alloy displayed crack initiation in persistent slip bands, followed by stage I and stage II crack propagation, respectively characterized by the occurrence of relatively featureless region and well defined striations upto 823K. At 823K, fine GS revealed ductile striations while medium and coarse grain sizes exhibited brittle striations (Figs. 4a & b). Brittle striations are the characteristic signatures of DSA process in fatigue. At 923 K, irrespective of GS, the oxidation effects became dominant. In fine GS, the effect of oxidation seems to result from the oxidation enhanced, stage I transgranular crack initiation and stage II transgranular crack propagation. The effect of oxidation on stage I cracking in planar slip alloys could be attributed to the slip step passivation mechanism, which by reducing the degree of slip reversibility enhances crack nucleation at slip steps. Oxide-enhanced transgranular crack growth results from the repeated formation of an oxide layer at the crack tip, its rupture, and exposure of the fresh material to the environment in each cycle. Oxidation at the crack tip would render a thin layer of material more brittle and so would assist crack propagation. In the medium and coarse grain sizes, build up of shear stress concentrations at the grain boundary triple points located at and near surface regions promoted oxidation induced intergranular cracking by grain boundary notching (Fig. 5a). The absorption and inward diffusion of oxygen atoms down the grain boundaries cause reduction in surface energy and, presumably, in the cohesive strength across the grain boundary. Occasionally, intergranular cavities have been noticed in all the grain sizes at 923 K (Fig. 5b). It is proposed that the cavities occur by the interaction of oxygen with grain boundary carbides. In spite of the presence of these cavities, fine GS did not undergo intergranular cracking. This can be related to the influence of GS on slip character. In medium and coarse grain sizes, planar slip bands cause edge dislocations to pile-up at grain boundaries, which promote stress concentrations. The cumulative action of stress concentration arising from slip band impingement leads to the unzipping of cavitated material. The ability of fine GS to spread the deformation inhibits the development of long pile-ups and associated stress concentration at the grain boundary, hence decohesion of the cavitated grain boundaries has not been achieved. Fatigue lives of various stainless steels decreased due to the increased tendency to form wedge cracks and cavities with increasing GS[2,18,19]. Grain size effects were found more pronounced under creep-fatigue interaction loading conditions[18,19].

2.2 Effects of Prior Cold Work on LCF Behaviour of Type 304 Stainless Steel

In the LCF tests conducted on 304SS employing total axial strain as the control parameter, cyclic deformation and lives were found to be a strong function of PCW. In general, SA material exhibited better total strain fatigue resistance than the material in 10, 20 and 30% PCW conditions in the range 300-1023 K, except for strain amplitudes less than 0.30% at 300 K[2,20-22]. At 823 K, LCF resistance decreased with increasing PCW (Fig. 6a). At 923 K, 10%PCW exhibited the lowest life; higher PCW levels showed recovery in life (Fig. 6b). At 823 K, the continuous decrease in life with increasing PCW has been found to have correlation with rank order

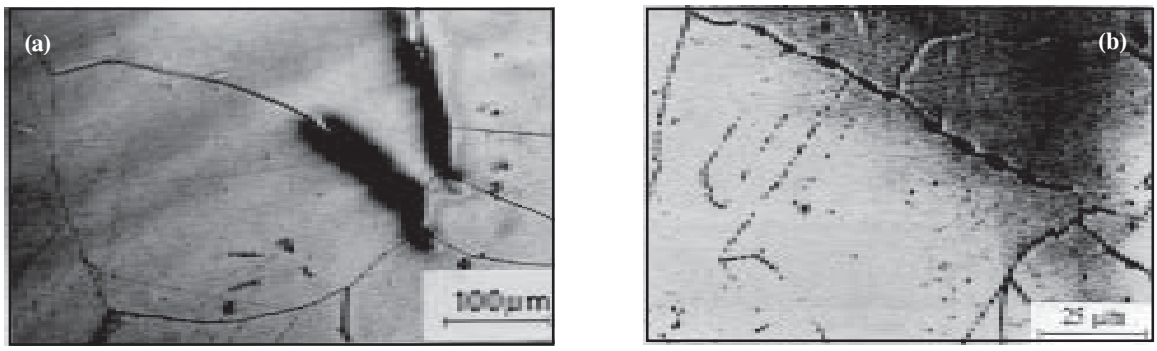

Fig. 5: (a) oxidation assisted intergranular cracking at grain boundary triple points and (b) Cavities on grain boundaries resulted by the interaction of oxygen with carbides[2].

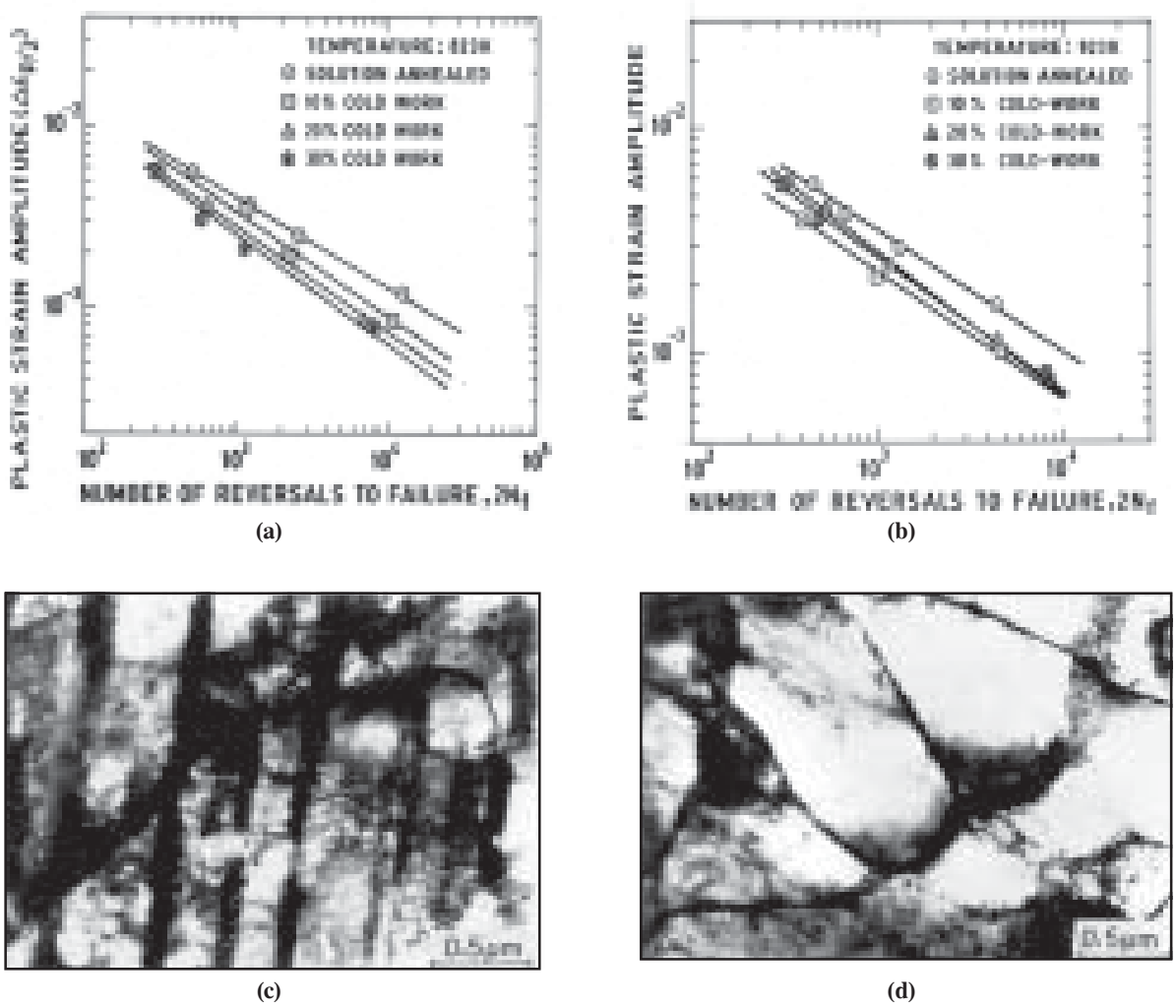

Fig. 6: Influence of prior cold work on fatigue life at (a) 823 K and (b) 923 K and substructures developed during LCF testing at (c) 823 K and (d) 923 K [2,20]

of monotonic ductility, which decreased continuously with increasing PCW. The improved life of 20 and 30% PCW materials at 923 K had its origin in strain induced precipitation and prevailing deformation modes. The 10% PCW alloy displayed intergranular cracking while 20 and 30% PCW conditions exhibited predominantly transgranular crack propagation. At 923 K, 10% PCW condition showed planar slip (Fig. 6c) while in 20 and 30% conditions the substructure primarily comprised cells and subgrains (Fig. 6d). Relatively large amounts intergranular carbides precipitated at higher PCW levels enhanced the resistance to grain boundary sliding and reduced the incidence of intergranular cracking. The dynamic recovery in 20 and 30% PCW conditions appears to lead to enhanced ductility with an associated increase in life. At 923 K, increase in LCF life at low strain amplitudes has also been observed in 20% cold worked 316L(N) stainless steel and titanium modified austenitic stainless steel (Alloy D9)[23-25]. The SA and 10% PCW 304SS displayed drastic reduction in life with decreasing frequency at 923 K[2,27]. Time dependent damage mechanisms namely inelastic deformation, DSA, oxidation, intergranular creep damage and uniform matrix cavitation have been found responsible for life degradation, however, their relative effects depended on initial microstructure and frequency. The exponent in plastic strain-life relationships showed more negative values in SA condition due to DSA effects while in the PCW alloy more positive values prevailed with decreasing frequency due to the beneficial effects associated with substructural recovery and intergranular precipitation.

Studies on Alloy D9 at 923 K clearly indicated the detrimental effect of cold work on creep-fatigue interaction resistance. Life decreased with increasing tensile hold time for both the alloy with Ti/C ratios of 4 and 8. Creep-fatigue interaction effects were more pronounced at higher Ti/C ratio due to profuse precipitation of TiC in matrix which promoted grain boundary weakening leading to intergranular failure.

2.3 Uniform Matrix Cavitation in High Temperature Fatigue

Studies on effects of microstructure on type 304 SS (presented in section 2.1 and 2.2) have led to the discovery of uniform matrix cavitation in strain controlled fatigue at elevated temperatures[1,2]. These voids were distributed uniformly within the grains without showing any special preference to heterogeneous nucleation sites like twin boundaries, slip bands, sub-grain boundaries or matrix carbides (Fig.7a)[29-32]. The existence of void free zones in the vicinity of grain boundaries have indicated that matrix voids nucleate without having any association with migrating grain boundaries (Fig. 7b). It was established that quenching the alloy from a very high solutionising temperature (to produce coarse GS) or prior cold working of the material is a necessary pre-requisite to cause homogeneous cavitation in the grain interiors during LCF deformation. The average void diameter (D) decreased with decreasing frequency (Fig. 7c) despite an order of magnitude increase in the total time available for nucleation and growth of voids. D increased with increase in strain amplitude (Fig. 7d) despite a considerable decrease in the time to failure at larger strain amplitudes.

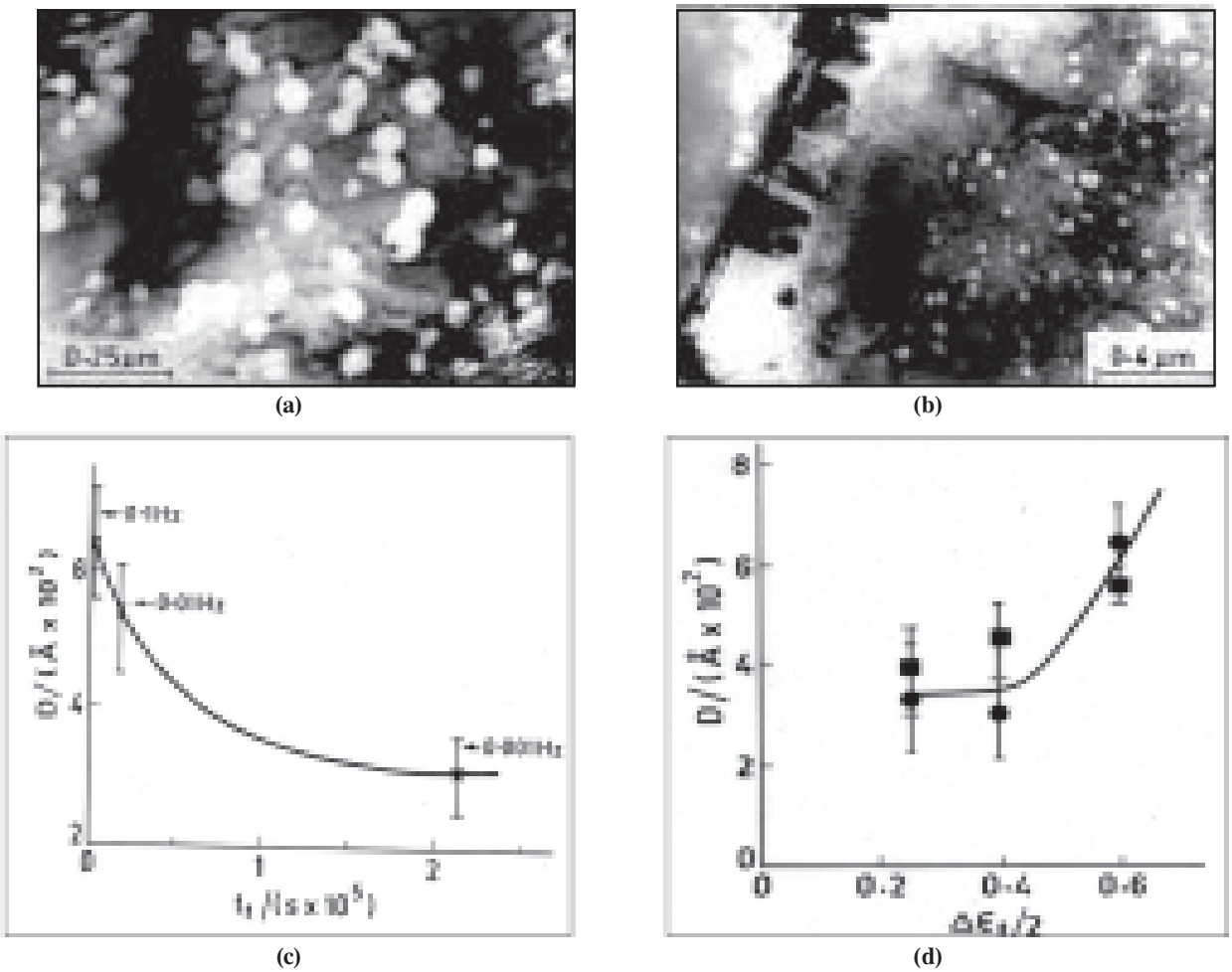

Fig. 7: (a) Uniform matrix cavitation during LCF, (b) Void free zone adjoining to grain boundary, (c) Variation of void diameter (D) with time to failure (t_f) for 10% cold work condition at 923 K and (d) Effect of strain amplitude on void diameter for 304 SS tested at 0.1 Hz at 923 K with two different PCW levels[2]

D has been found to increase with PCW. It has been proposed that cyclic deformation under favorable conditions generate large number of matrix voids and D is controlled by production of excess lattice vacancies (higher at higher strain amplitudes and high frequencies) and by their probability of arrival at the "void embryo" rather than the time available for growth. Interrupted tests revealed an incubation period for the nucleation of matrix voids. During this period the cumulative accumulation of vacancies generated during PCW and early cyclic deformation build up to a level high enough to cause direct condensation on effective nucleation sites such as dislocation loops. There was no significant increase in the size of voids between 20% and end of life, whereas the number density increased substantially. The development of intergranular creep cavities, their subsequent growth and linkage which lead to intergranular fracture have been well established. The interaction of propagating fatigue crack with intergranular cavities leads to creep-fatigue interaction failures. Uniform matrix cavitation is now considered as a possible damage mode in fatigue.

2.4 Effects of Prior Microstructure on LCF Deformation and Fracture of Superalloys Nimonic PE 16 and Inconel 718

The cyclic deformation and fracture behaviour of Nimonic PE-16 superalloy has been assessed in various microstructural conditions and micromechanisms influencing the fatigue behaviour have been identified[33-35]. Three different microstructures employed for LCF testing include : (A) A fine grain structure free from carbides and γ′, (B) microstructure with intra and intergranular $M_{23}C_6$ and uniform distribution of spherical and peak aged γ′ of 18 nm diameter, and (C) microstructure with predominantly intergranular MC and overaged γ′ of 35 nm diameter. Microstructures B & C were produced through double ageing treatments and were shown to have a good combination of tensile strength and ductility[36-38]. Alloy A exhibited higher plastic strain fatigue resistance than B and C[36]. The peak aged alloy B revealed a non-ideal plastic strain fatigue response with a discontinuity in the strain-life plots (Fig. 8a); the samples cycled at lower strain amplitudes exhibited much shorter lives than would be predicted by extrapolation from the high plastic strain amplitude portion of the plot. Alloy B also exhibited two stages in its half-life cyclic stress-strain curve (Fig. 8b). The fatigue life and fracture behaviour have been found to depend on the nature of slip, distribution of γ′ and intergranular carbides. Alloy A in which the deformation occurred by planar slip (Fig. 9a) exhibited better fatigue resistance while the microstructure C in which γ′ particles were bypassed predominantly by Orowan looping mechanism displayed the least (Fig. 9b). The beneficial effects of planar slip on life results from the slip reversibility which retards the transgranular crack initiation and propagation. Since bypassing of γ′ particles by Orowan mechanism requires cross slip and loop formation, slip was not reversible to the same extent as in the cutting process

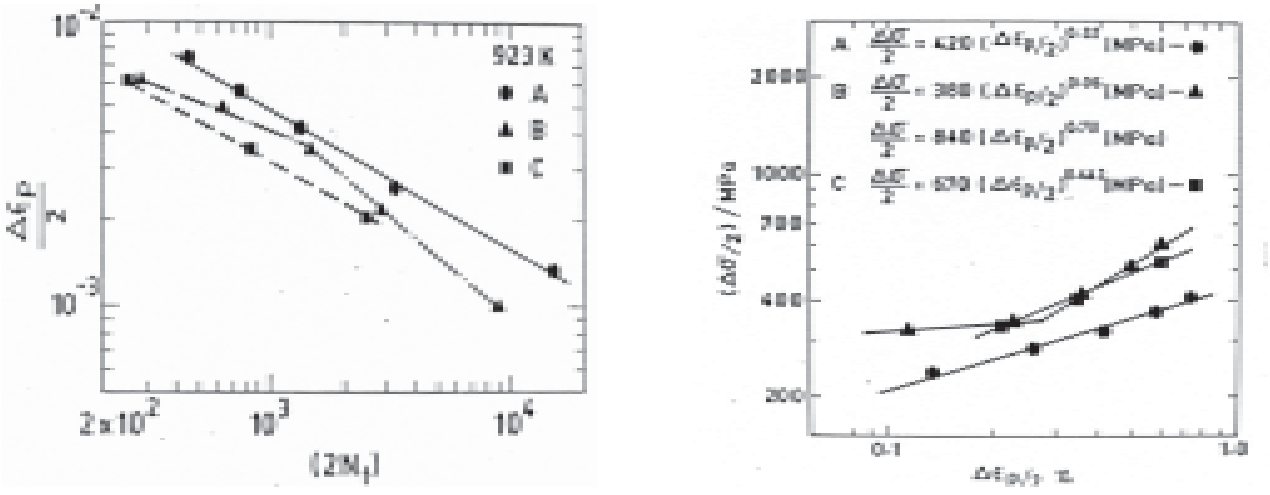

(a) (b)

Fig. 8: (a) Coffin-Manson plots and (b) Cyclic stress-strain curves of Alloy A, B & C at 923 K[33,34]

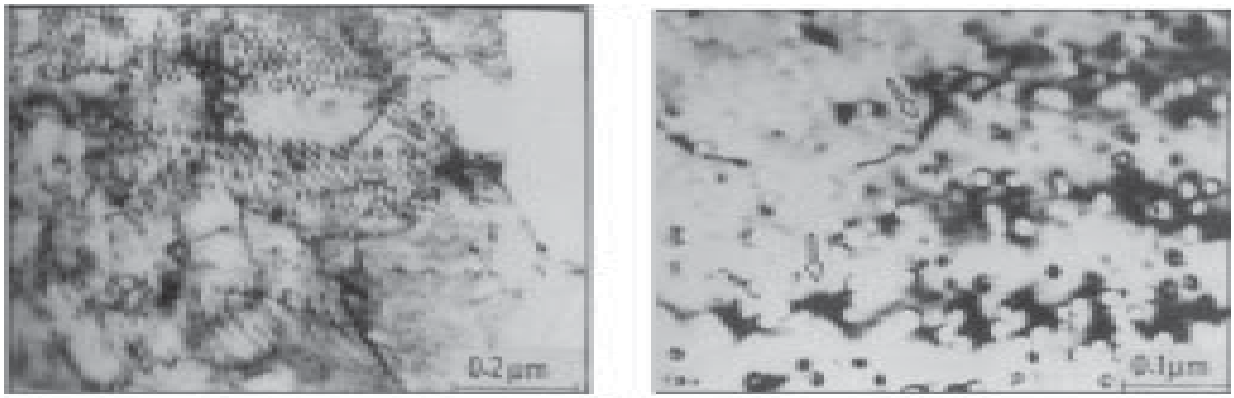

(a) (b)

Fig. 9: (a) Planar dislocation arrangement in Alloy A at a strain amplitude of +0.4% and (b) Orowan looping mechanism in Alloy C at a strain amplitude of +1.0%[34]

and promotes accelerated propagation of fatigue cracks. Alloy C exhibited pronounced transgranular cleavage fracture in addition to some intergranular cracking (Fig. 10a). The cleavage fracture was associated with widely spaced slip bands in which channelization of dislocation activity has occurred (Fig 10b). The channelization of deformation leads to dislocation pile-ups at the grain boundaries, causing stress concentration and intergranular decohesion of the carbides. The discontinuity in strain-life curves of alloy B resulted from the differences in the degree of homogeneity of deformation and fracture modes between low and high strain amplitudes. In alloy B, high strain amplitudes caused homogeneous deformation and transgranular fracture while concentrated deformation in slip bands and mixed trans plus intergranular mode of fracture prevailed at low strains. The beneficial effect of planar slip was eclipsed under the double aged conditions where the initial and evolving microstructure contained shearable γ′ precipitates, which promoted strain localization.

The deformation mechanisms and fatigue behaviour of double aged and pre-strained Inconel 718 superalloy were investigated at room temperature[39,40]. The prestrains investigated simulate those imposed on materials during proof testing, accidental overload and autofrettage. The alloy softened after a small amount of hardening during the initial cycles (Figs.11a & b). At a strain range of 2%, monotonic tensile straining did not have a significant effect on the subsequent fatigue life. At lower strain range, the fatigue life of 10% pre-strained alloy was lower by nearly factor of five. Dislocation pairs observed in the slip bands indicated that ordered γ″ precipitates were sheared during deformation process (Fig. 12a). Cyclic softening was attributed to the continuous "mechanical scrambling" of γ″ precipitates by

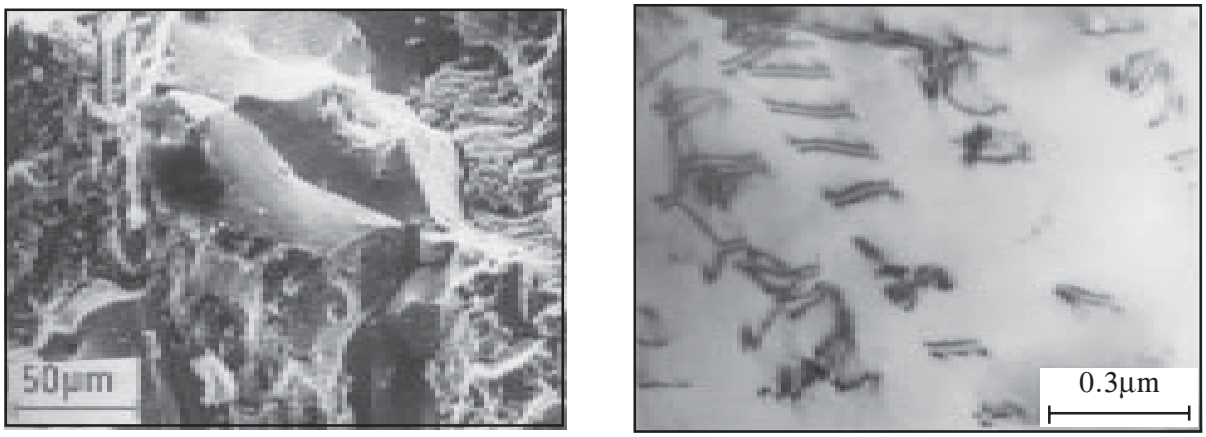

(a) (b)

Fig. 10: (a) Facetted fracture appearance and (b) Superdislocation pairs in Alloy C at 923 K[34]

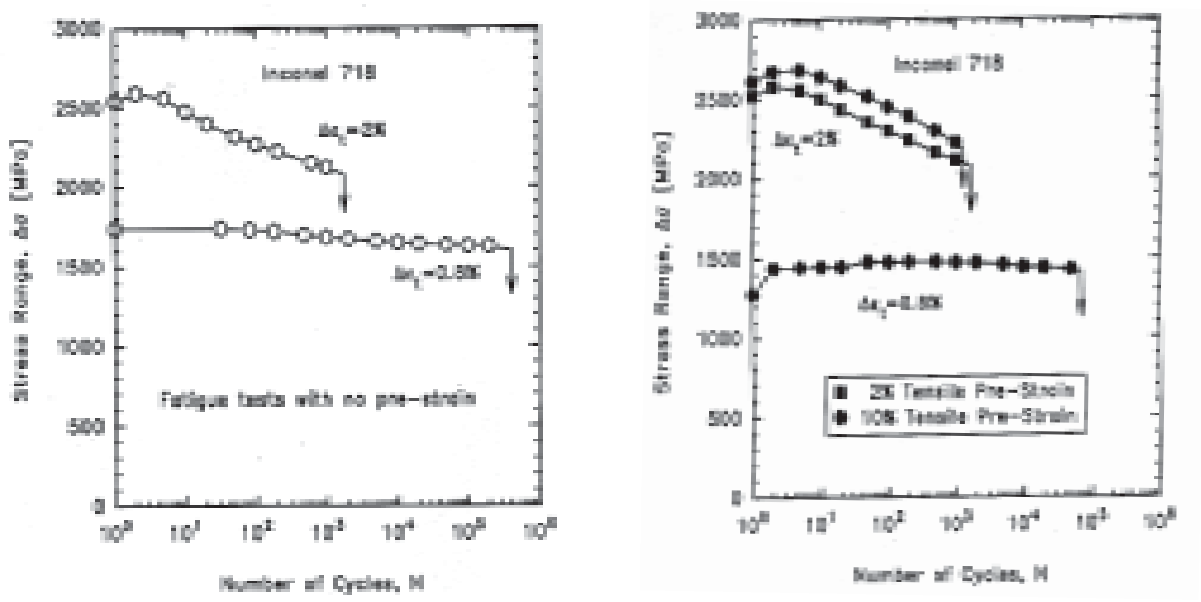

(a) (b)

Fig. 11: Evaluation of cyclic stress range in a fully reversed fatigue test (a) with no pre-strain and (b) with pre-strain[39,40]

dislocations in deformation bands, which eventually led to the formation of precipitation-free deformation bands (Fig. 12b). In specimens that were monotonically strained in tension followed by fatigue testing, deformation during the fatigue part of the test occurred mostly along the deformation bands activated during the monotonic tensile strain.

3. EFFECTS OF DYNAMIC STRAIN AGEING ON LCF BEHAVIOUR OF STAINLESS STEELS

Table 1
CYCLIC STRESS AND CYCLIC PLASTIC STRAIN VALUES FROM EXPLORATORY STRAIN CONTROLLED LCF TESTS[2]

Total Strain Range	Temperature (K)	Stress Amplitude (MPa)		Plastic Strain Range (%)
		First Cycle	Saturation	
0.80	673	141	248	0.469
0.80	773	143	270	0.460
0.80	823	173	278	0.453
0.80	873	160	228	0.498
0.80	923	159	224	0.523

In the last two decades, considerable research efforts have been devoted to characterize the effects of Dynamic Strain Ageing (DSA) on LCF behaviour of austenitic stainless steels 304, 304L(N), 316L(N), Alloy D9, ferritic steels 2.25Cr-1Mo, 9Cr-1Mo, Mod. 9Cr-1Mo and superalloys Nimonic PE-16 and Inconel 718 at IGCAR, Kalpakkam. The temperature range of application of these alloys encompass the domain of occurrence of DSA. The early investigations on type 304 SS provided answers to several probing questions. The characteristics of DSA in 304 SS during LCF were evaluated as a function of grain size (75, 310 and 700 μm), temperature (300-923K), frequency of cycling (0.0005-1.0 Hz) and strain range (0.5-3.0%)[2,41]. Through exploratory LCF tests, the peak DSA temperature was established as 823K. At 823K, DSA was manifested as a peak in the tensile saturation stress, a minimum in the plastic strain generated in the cycle (Table 1), and increased cyclic hardening rate. These features were found to be analogous to the behaviour in monotonic tension tests where a peak in flow stress, minimum in tensile ductility and increased work hardening rate were observed. Over the DSA temperature range serrations were seen in the plastic portions of stress-strain hysteresis loops; the type and magnitude of serrations were found to depend on grain size, applied strain amplitude, test temperature and frequency of cycling. The critical temperature for the onset of serrations was established

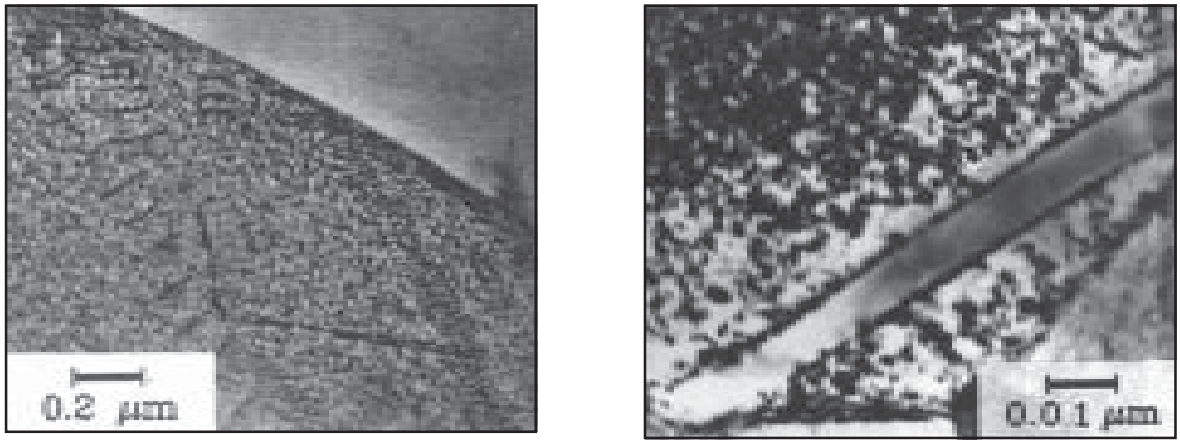

(a) (b)

Fig. 12: (a) Slip band, dislocation pairs and pile-up at a grain boundary $\Delta\varepsilon_t = 0.8\%$ and (b) Deformation bands devoid of precipitates[39,40]

to be lower in LCF than in monotonic tensile deformation. Fatigue life decreased drastically with decreasing strain rate (Fig. 13a)[2,6,41,42]. Further over the DSA regime half-life stress amplitude showed a negative strain rate sensitivity and this occurred earlier than the appearance of serrations in the stress-strain hysteresis loops[2, 42]. Furthermore, phenomenologically DSA corresponded to a change in cyclic life exponent 'c' in Coffin-Manson equation $\Delta\epsilon_p/2 = \varepsilon_f' (2N_f)^c$ (Fig. 13b). DSA was found to increase the inhomogenity of deformation during fatigue, leading to brittle intergranular decohesion resulting from the impingement of persistent slip bands on grain boundaries (Fig. 14)[2, 42]. The medium grain size exhibited greatest tendency for brittle intergranular decohesion[2,6,43]. The detrimental effect of DSA on LCF life has also been noticed in the studies conducted on stainless steels Alloy D9[44,45], 304L(N)[46] and 316L(N)[47-50] and Nimonic PE-16[8] superalloy in the range 298-923K. The operation of DSA introduced critical changes in the cyclic stress response and dislocation substructure in the studies performed on 304 SS, 304L(N), Alloy D9 and 316L(N). The dislocation structure transformed from cells symbolizing the wavy slip character at low temperatures to a predominantly planar slip in the temperature range where DSA occurred and became wavy again at higher temperatures. The effects of

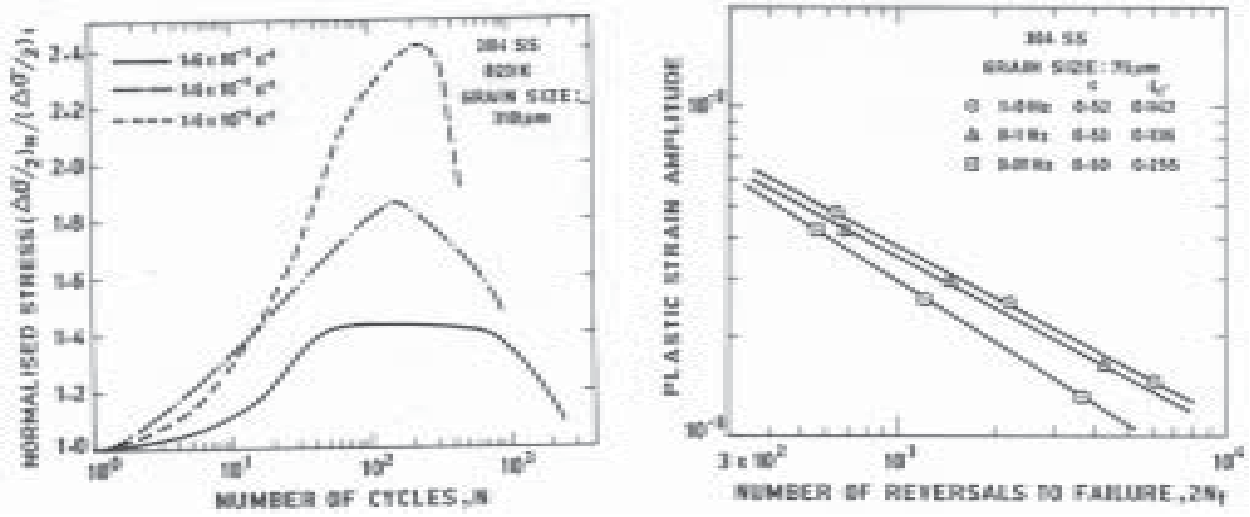

(a) (b)

Fig. 13: (a) Normalised cyclic hardening curves illustrating the influence of strain rate 823 K for medium grain size material, strain amplitude +0.4% and (b) Coffin-Manson plots for fine grain size at 923 K for different frequencies[2].

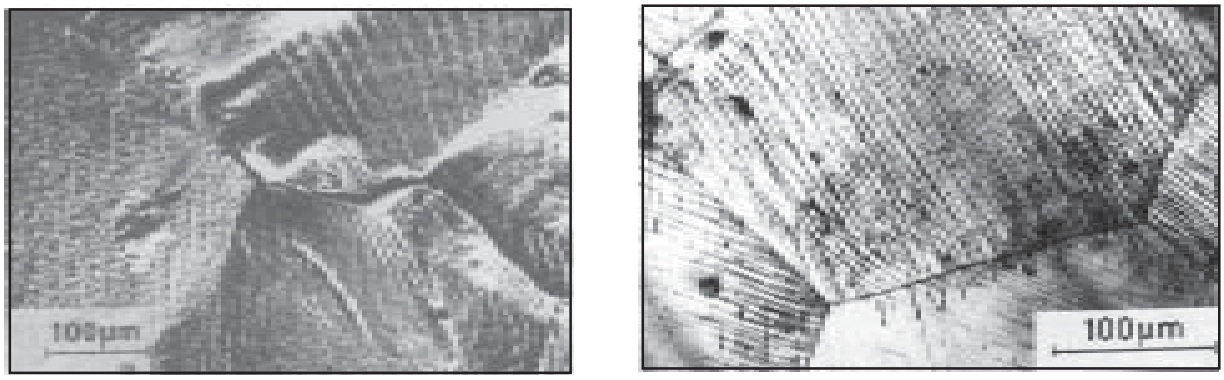

(a) (b)

Fig. 14: (a) Intergranular decohesion due to impingement of slip bands and (b) Very high density of planar slip bands in the surface connected grains of sample tested at 923 K[2].

DSA were explored in Alloy D9 as a function of Ti/C ratio. The Alloy D9 with a Ti/C ratio of 8 exhibited more detrimental effects on life due to DSA than the alloy with Ti/C ratio of 4. The lower critical temperature for commencement of DSA was reduced with increasing Ti/C ratio.

3.1 Cyclic Deformation Behaviour of Superalloys

The changes in peak tensile strain amplitude with the number of cycles at various temperatures in the range 298-1273 K (25-1000°C) for a solid solution hardened cobalt base superalloy are shown in Fig. 15[5, 51]. The temperature dependent stress response can be considered in three general domains, these are low (298-573 K), mid (623-973 K) and high (≥1023 K), where the mid temperature regime represents DSA domain. In the DSA domain the cyclic deformation was characterized by cyclic hardening with a peak at 923 K. The maximum tensile stress developed during the LCF tests decreased initially with increasing temperature to 573 K, displayed an increase with increasing temperature in the range 673-923 K and then showed rapid fall above 923 K. Concurrently, there was a gradual reduction in the inelastic strain pertaining to the cycle at half-life with increasing

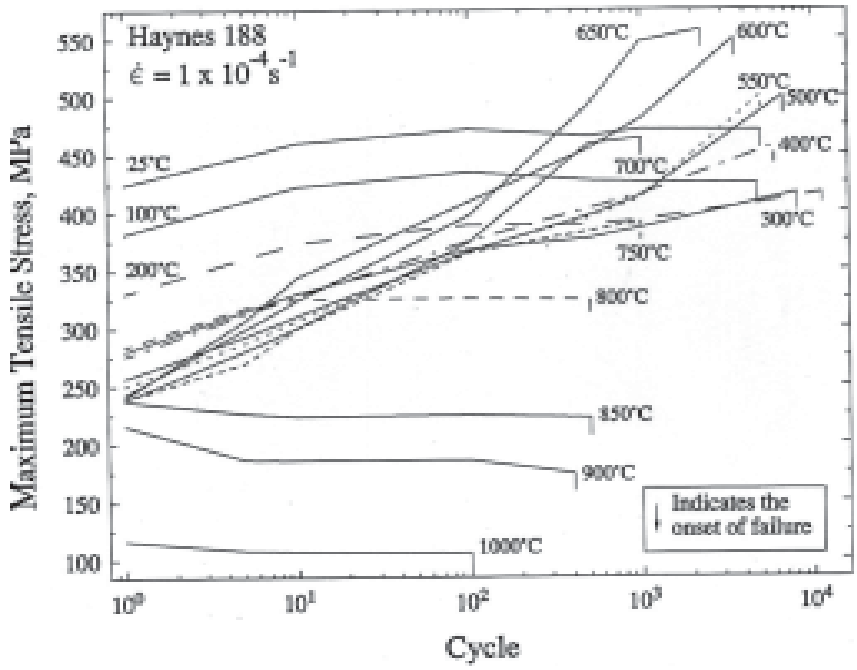

Fig. 15: Cyclic stress response curves for Haynes 188 superalloy at various temperatures[5]

temperature in the range 573 to 923 K. These observations confirm that DSA occurs in the alloy in the intermediate temperature domain. The instantaneous strain rate dependence of cyclic stress has been examined by conducting exploratory strain-rate change tests on companion specimens in the low, intermediate and high temperature domains (Fig. 16). These tests were performed by only periodically decreasing the strain rate to 10^{-4} s^{-1} for one cycle and then returning to the higher strain rate. Stress response plots indicated that the macroscopic Strain Rate Sensitivity (SRS) is positive below 573 K, strongly negative between 673 and 923 K, and only slightly negative at 973 K. SRS was completely positive above 973 K.

In the low temperature range (below DSA domain) the substructure was composed of dislocation bundles while in high temperature regime (above DSA domain), the occurrence of dynamic recovery by thermally activated climb led to the formation of sub grains. In the DSA domain, between 673 and 823 K, dislocations frequently formed planar arrays and extensive dislocation pile-ups at the grain boundaries (Figs. 17a&b). A large number of dislocations in planar slip bands at 673 K showed stacking fault fringe contrast and many were dissociated into stacking fault ribbons. The propensity for formation of stacking fault ribbons reached a peak at 823 K (Fig. 17c). Towards the end of the DSA regime, at 873 and 923 K, dislocation density was relatively high (Fig. 17d). These results clearly confirmed that the deformation occurs by planar slip in the DSA domain. When DSA operates, in order to maintain the imposed strain, additional dislocations are generated leading to the observed increase in dislocation density. In the circumstances where the planar slip is the predominant mode of deformation, the marked cyclic hardening likely results from the combined effects of accumulation of dislocations in planar slip bands, uninterrupted initiation of slip bands until the maximum stress is attained, and the progressive build-up of dislocation pile-ups during cycling. The high dislocation density in planar slip bands could arise from the diminished tendency for the annihilation of dislocations through the difficulty of cross slip induced due the immobilization of dislocations due to solute locking. The continuous hardening together with the absence of saturation stress stage between 573 and 823 K, where planar slip is the predominant mode of

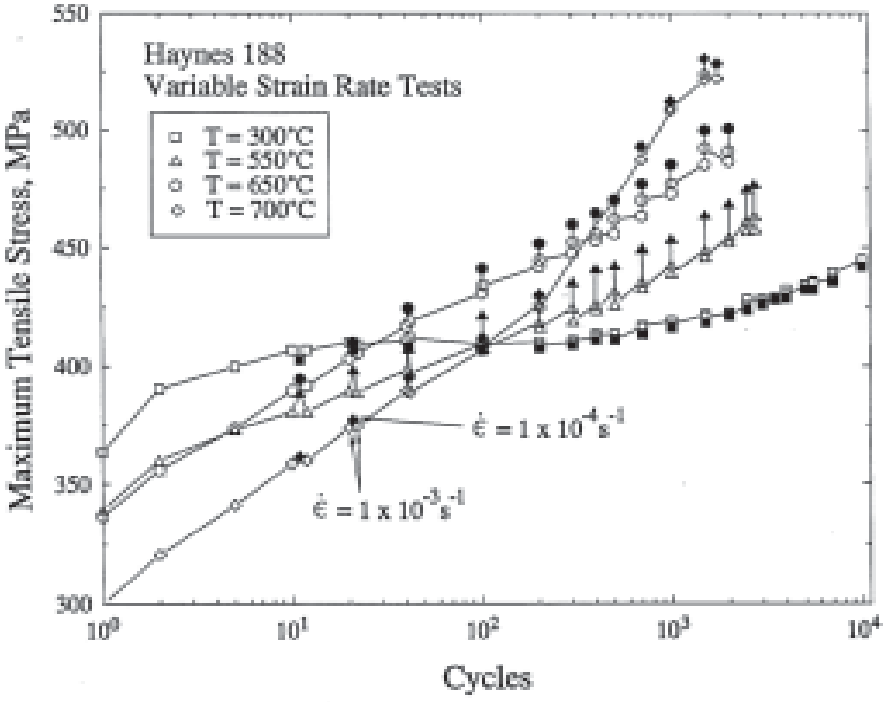

Fig. 16: Instantaneous strain rate change tests at various temperatures to identify the strain rate sensitivity of cyclic stress in Haynes 188 Superalloy[5]

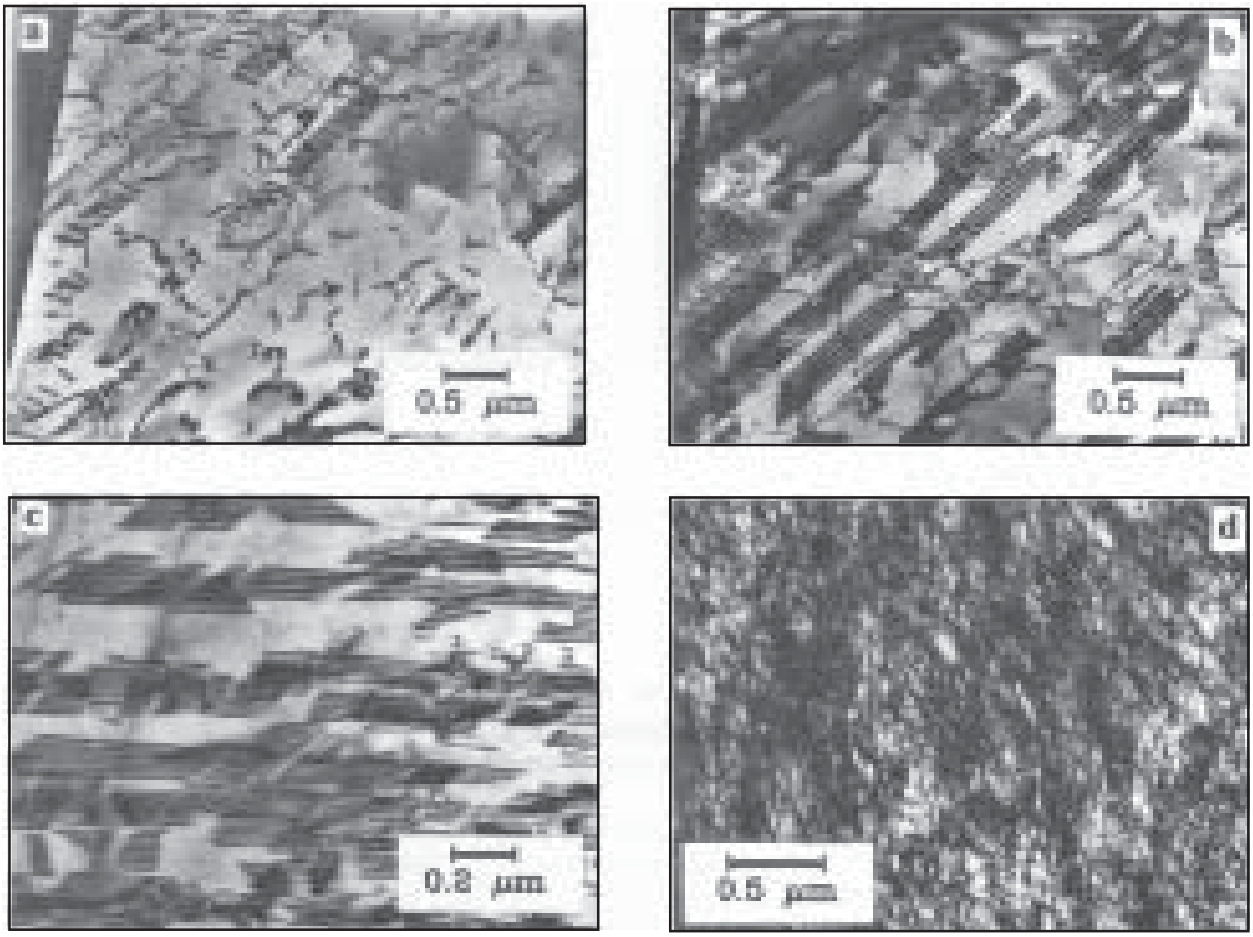

Fig. 17: (a) Dislocation pile-ups and stacking fault fringes in planar slip bands at 400 °C, (b) Planar arrays of dislocations and stacking fault in slip bands, (c) high density of stacking faults at 550 °C and (d) dislocations in the form of networks at 650 °C[51]

deformation can be attributed to the difficulty of annihilating dislocations. The effect of annihilation of dislocations is reflected by reduced degree of cyclic hardening between 1023 and 1123 K. The dynamic recovery, which was manifested in the form of sub grain formation above 1123 K, however, completely suppressed cyclic hardening. At room temperature, serrated flow has been observed in Inconel 718 superalloy in solution annealed and double aged conditions. The back stress exerted by accumulated parallel pile-up of dislocations in planar slip bands and subsequent relaxation of internal stress by initiating new plastic flow in adjacent grains was proposed to be cause of serrated flow in IN 718 at room temperature[52].

4. THERMOMECHANICAL FATIGUE BEHAVIOUR OF STAINLESS STEELS AND SUPERALLOYS

4.1 TMF Behaviour of 316L(N) Stainless Steel[53]

Detailed investigations have been performed to understand the TMF behaviour of 316L(N) Stainless Steel used in FBRs. The feasibility of generating reliable TMF deformation and life data was established by conducting several exploratory tests under in-phase (wherein the maximum temperature and peak tensile strain coincide) and out-of-phase (maximum temperature and peak compressive strain coincide) testing conditions (Fig. 18). Exploratory tests were conducted to optimize the sample design,

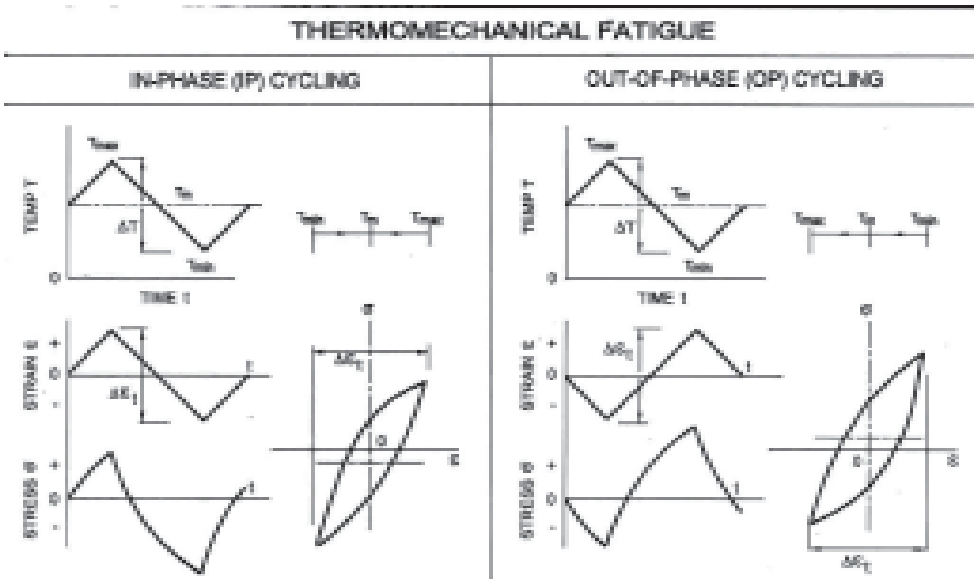

Fig. 18: Schematic waveforms employed in TMF testing

configuration of induction coils and appropriate heating and cooling rates in order to reduce the temperature gradients in the sample at the strain and temperature reversals of the TMF cycle. A procedure was established to ensure proper phasing between temperature and mechanical component of the strain by providing thermal strain compensation as a function of real-time specimen temperature, which involved subtraction of thermal strain from total strain during TMF test on a real-time basis and establishing the mechanical strain as the controlling parameter. The studies on austenitic stainless steels revealed that the mechanical strain rate shall be kept $\leq 6.4\times10^{-5}$ s^{-1} in order to avoid the serious temperature gradients in the test specimens at the strain reversals. Both IP and OP TMF tests were carried out on 316L(N) austenitic stainless steel on cylindrical hollow tubular samples using different mechanical strain amplitudes in the range, $\pm$ 0.25% to $\pm$ 0.6% at a constant strain rate of 6.4×10^{-5} s^{-1}. The temperature cycles employed consisted of two different categories namely (a) an identical temperature range with increasing peak temperature (300-550, 350-600, 400-650°C) and (b) a constant peak temperature with increasing temperature range (400-600, 350-600, 400-650, 350-650°C).

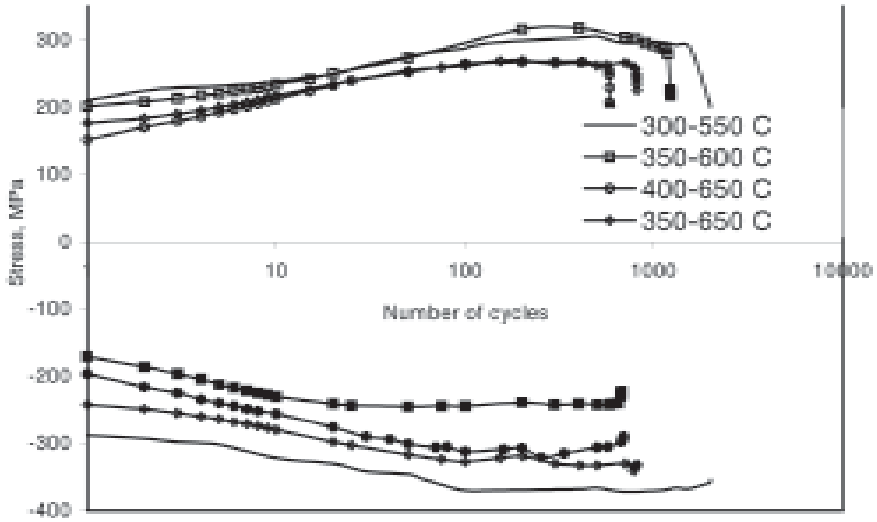

Fig. 19: Cyclic stress response obtained under TMF-IP and LCF cycling, $\Delta\varepsilon_{mech} = \pm0.4\%$[53]

In both IP and OP conditions the fatigue life decreased with increase in peak temperature of the TMF cycle at constant temperature interval (Fig. 19)[53]. As the peak temperature of TMF cycle was increased, the differences in lives of IP and OP tests were narrowed down (Table 2). TMF life in out-of-phase cycling was lower than that in the in-phase tests in the low temperature regimes (Fig. 20), while in the creep temperature regime, the IP tests yielded lower lives. With the peak temperature kept constant in the creep range (650°C), and increasing the lower temperature of TMF interval (350 to 400°C), the fatigue life decreased both in IP and OP conditions (Table 2). The differences in IP and OP tests increased with reduction in strain amplitude.

Table 2

TMF AND LCF LIFE DATA ON 316L(N) STAINLESS STEEL AT VARIOUS TEMPERATURES ($\Delta\varepsilon_{MECH} = \pm 0.4\%$)

Temperature range, ΔT °C	TMF life		Isothermal LCF life at maximum temperature (T_{max})
	In-Phase	Out-of-Phase	
300-550	2093	1312	693
350-600	1210	1000	835
400-650	585	853	672
400-600	1221	709	835
350-650	811	1256	672

Crack initiation and propagation was transgranular in both IP and OP conditions when the peak temperature of TMF cycle was less than 600°C (Fig. 21a). In the tests with the peak temperature at 650°C, OP tests displayed transgranular fracture while mixed trans plus intergranular mode of fracture occurred in IP tests (Fig. 21b). Influence of creep on the TMF damage was evident in the form of extensive intergranular cracking in the 400-650°C IP test. The relatively higher stress response seen under OP cycling in the lower temperature regimes shortened the crack initiation and propagation lives contributing to the overall reduction in life. At very high temperatures, IP cycling proved to be more deleterious as a consequence of a creep-dominated intergranular cracking intersperced with oxidation effects. Influence of oxidation was more prominent in the IP tests as a consequence of the cracks remaining open at the high temperature end of the TMF cycle, thereby allowing easy environmental access to the crack tip. The isothermal tests conducted concurrently at the peak temperatures employed in TMF cycles (550°C and 600°C) displayed lower lives compared to both IP and OP tests (Table 2). The IP and OP TMF lives (400-650°C) were lower than isothermal lives observed at 650°C.

4.2 Dynamic Stain Ageing Effects in TMF of Superalloys[54-58]

The effects of DSA on TMF behaviour have been explored by conducting detailed investigations on

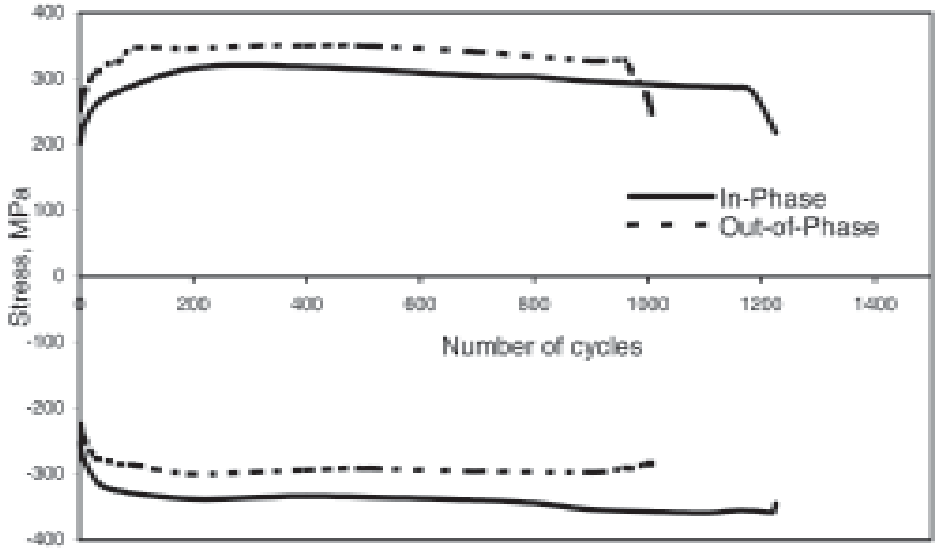

Fig. 20: Comparative stress response: IP and OP cycling at, $\Delta\varepsilon_{mech} = \pm 0.4\%$[53]

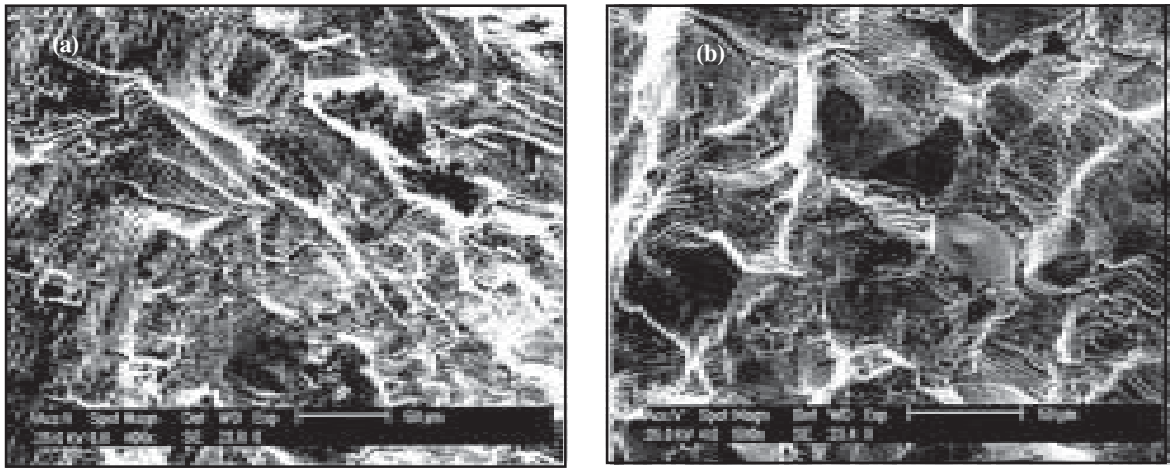

Fig. 21: (a) Oxidation-assisted mixed mode cracking under 400-650°C IP cycling, (b) SEM fractograph showing creep-dominated IG cracking interspersed with clearly defined striations in 316L(N) stainless steel

Haynes 188 Superalloy in four temperature intervals (ΔT = 350-550, 400-650, 500-750 & 600-850^{0}C). In this alloy DSA was found to occur over a wide temperature range between approximately 400 to 700^{o}C[5]. In the TMF test with ΔT = 350-550^{0}C, the maximum and minimum temperatures were within and below the DSA range, respectively (for a strain rate of 10^{-4} s^{-1}), while in the 500-750 and 600-850^{0}C tests the maximum and minimum temperatures were above and within the DSA range respectively. The test with ΔT = 400-650^{0}C is entirely within the DSA range. The evolution of tensile and compressive stresses under IP TMF conditions with various temperature intervals are summarized in Fig. 22, tensile stress response curves of selected isothermal tests are also shown to facilitate comparison. It must

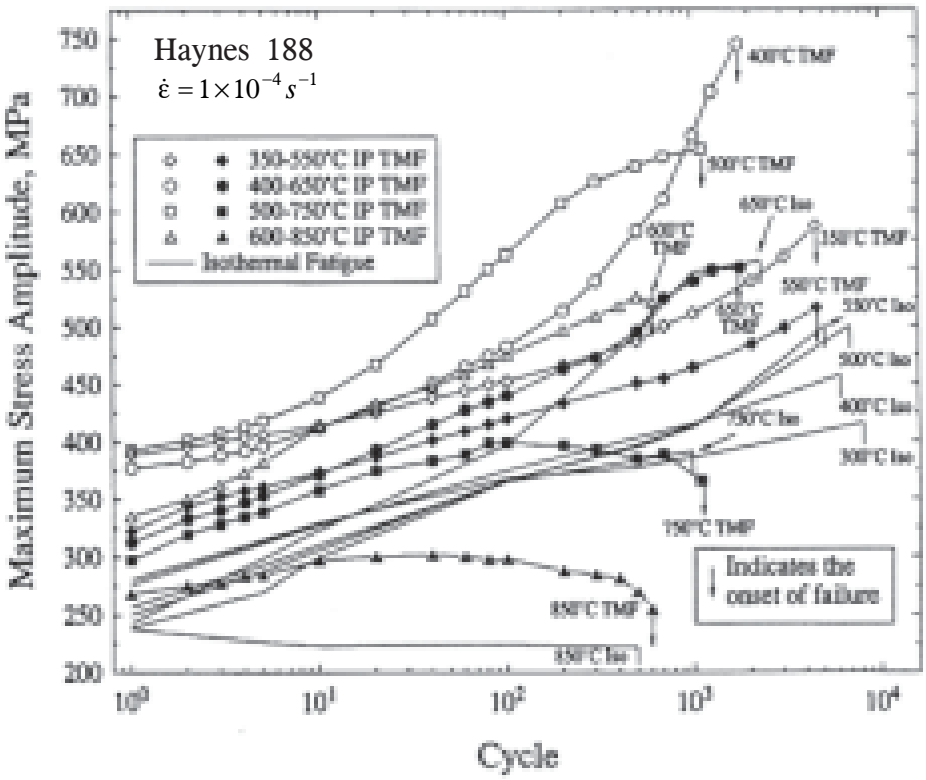

Fig. 22: Cyclic maximum stress amplitudes of TMF and LCF with $\Delta\varepsilon^m$ = 0.8% and strain rate = 10^{-4} s^{-1}

be mentioned that each TMF test is represented by two curves, one showing the stress amplitude at the maximum temperature and the other showing the stress amplitude at minimum temperature. Further, for viewing simplicity, all stress amplitudes are shown as being positive (tensile) whereas in IP tests, the minimum temperature amplitude shown corresponds to compressive stress. In the isothermal fatigue tests, tensile and compressive stress amplitudes in any given cycle were essentially equal, whereas in the TMF tests, mean stresses developed as a consequence of the dynamic temperature conditions. IP TMF tests developed a compressive mean stress, that is, the compressive stress amplitudes were higher than the tensile stress amplitudes, whereas OP TMF conditions led to tensile mean stresses. The mean stress was mild in the 350-550^{0}C test, however, the other TMF tests experienced significant mean stresses which generally tended to increase with cycling. The mean stresses developed were particularly large when the maximum temperature of the TMF cycle was above and the minimum temperature was within the DSA range. This result was due to the fact that DSA enhanced hardening was prevalent at one extreme of the cycle and softening due to the thermal recovery effects was prevalent at the other extreme.

In all the TMF tests, the maximum stresses achieved just prior to the onset of failure at the maximum temperatures of the cycles were almost identical to those attained in corresponding isothermal tests; however, the number of cycles needed to attain the maximum in each of the TMF tests was less than those in the isothermal tests. In contrast, the maximum stresses achieved at the minimum temperature extremes in the TMF tests were not well represented by the isothermal tests performed at corresponding temperatures. This may suggest that the TMF macroscopic behaviour is most influenced by the substructural features associated with the peak temperature.

In general, the lower temperature peak stresses experienced greater increases in the TMF tests showing significant deviations from the corresponding isothermal tests. This effect was most pronounced in the tests conducted with a temperature interval of 400-650^{0}C. The maximum hardening rates and magnitudes experienced by the 400^{0}C TMF peaks far exceeded those displayed isothermally at 400^{0}C. This indicates that the TMF stress hardening at 400^{0}C could not have been anticipated from the isothermal data. Further the stress values achieved far exceeded (by 25 to 35%) than those experienced isothermally at 650^{0}C. This is a significant result considering that the 650^{0}C isothermal values represent the maximum for the entire isothermal data base. This isothermally unbounded behaviour is clear evidence of thermomechanical path dependence, as the material behaviour observed at 400^{0}C is profoundly influenced by the deformation substructure developed over the full ΔT. Although the minimum temperature peak stresses in the 500-750^{0}C cycle showed the excessive increase due to DSA effects when compared to the isothermal tests at 500^{0}C, the amount of hardening was far less than that obtained in the 400-650^{0}C TMF tests, because part of the cycle remained in the range where thermal recovery effects became operative. In the TMF tests with ΔT = 600-850^{0}C, where the main fraction of the cycle involves loading above the DSA range, it is apparent that the thermal recovery effects have become substantial, causing the hardening mechanisms associated with DSA to be less effective at the lower temperature extreme of the cycle.

5. DEVELOPMENT OF FATIGUE DESIGN CURVES FOR THICK SECTION FORGINGS OF 9CR-1MO FERRITIC STEEL[59-61]

Advances in steam cycle conditions of the FBRs to withstand temperatures upto 823 K depend on the ability to process and fabricate heavy section components from ferritic steels such as 9Cr-1Mo and its derivatives. Steam generators require massive tube plates to operate continuously at temperatures upto 793 K. LCF and creep-fatigue data base for ferritic steels for sections beyond 32mm is not available and the guidelines for the fatigue design have not been given until recently for thick section ferritic alloys in any of the codes. Investigations were conducted on 300 mm thick 9Cr1Mo tube plate to examine whether the LCF data available on thin section bar and sheet materials could be adequately utilized for the design of thick-section components in the range 723-793 K[59-61]. The alloy in simulated post weld heat treatment condition exhibited predominantly cyclic softening (Fig. 23a). Total strain LCF resistance of

thick section tube plates of 9Cr-1Mo was inferior to that of hot rolled thin sections tested in either normalized plus tempered or in simulated thick-section heat treatment conditions (Fig. 23b) owing to its coarse grain size. Within the range of strain amplitudes examined, the experimental data on fatigue life at elevated temperatures were found to match well with the LCF lives predicted by the Tomkins crack growth model. All the important parameters required for life prediction using Tomkins crack growth equation were deduced from the deformation and fracture characteristics obtained on the alloy during tension and LCF tests at various temperatures on thick section material. The total strain-life relationship comprising of Basquin and Coffin-Manson equations was employed to extrapolate the experimental fatigue curves upto 2×10^6 reversals. Using the fatigue data generated on small specimens and employing the philosophy embodied in the ASME code case N-47, fatigue design curves have been developed for thick section 9Cr-1Mo steel. The extrapolated fatigue curves were used to construct tentative fatigue design curves by applying a reduction factor of 20 on the number of reversals or a factor of two on the strain amplitude (Fig. 23c). These factors cover effects such as environment, size, surface finish and scatter of the data. It was generally observed that at low strain amplitudes division of the strain amplitude by a factor

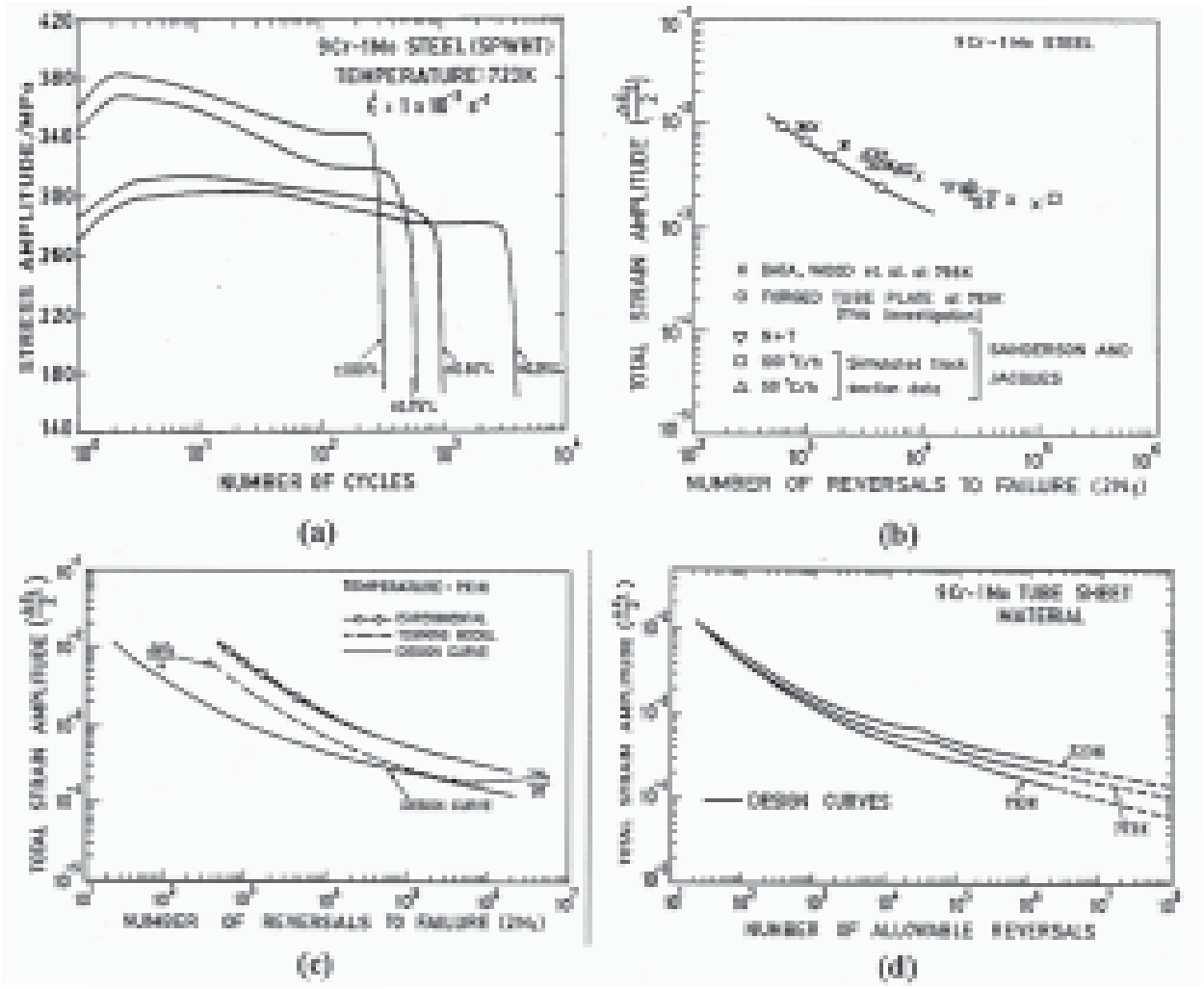

Fig. 23: a) Cyclic stress response curves at 793 K, b) Fatigue endurance data of 9Cr-1Mo steel on thick section forged tube plates and thin section hot rolled bars for different heat treatment conditions, c) Experimental and predicted curves of total strain amplitude against number of reversals and the fatigue design curve at 793 K and d)Fatigue design curves at different temperatures[60]

of two gave the lowest curve, while at high strain amplitudes a reduction of factor of 20 on the number of reversals yielded the lowest curve. The more conservative of the two estimates in the different segments were joined together to obtain the fatigue design curves for continuous cycling for the temperature range 723-793 K (Fig. 23d). In order to obtain the design curves beyond 2×10^6 reversals, an extrapolation technique following the French design code RCC-MR was adopted. A fatigue design curve applicable for the temperature range 300-644 K was computed based on room temperature tensile properties, incorporating the concept of fatigue limit and mean stress.

6. FATIGUE BEHAVIOUR OF STAINLESS STEEL WELDMENTS

Often, fracture in fabricated engineering structures initiates at welded joints. The welding process produces local microstructural changes that are seldom considered in the operation design analysis. The metallurgical condition of the material is changed; local residual stresses of magnitude well beyond the component design stress may be introduced and frequently defects are produced during the welding process which sometimes go undetected. These defects together with unfavourable design geometries provide further stress concentrations, The combined effects of these on LCF behaviour are often overlooked by the designer, fabricator and user of the components. Failures in the welded joints are prevented through the use of safety factors on stresses and strains and by requiring the welds to be located in the regions of relatively low stresses. In the absence of substantial information on welds, ASME boiler Vessel code Case N-47 imposes a limit on the design strains in the weld regions at one-half of the value permitted in the base metal for applications at elevated temperatures where creep effects are significant. The allowable number of fatigue cycles is also one-half of the value permitted for the parent metal. There is a serious concern about the conservatism introduced in the design rules. In austenitic stainless steels the δ-ferrite introduced to reduce their tendency to hot cracking gets transformed to brittle σ-phase when these materials are exposed to elevated temperatures for extended periods of time. The transformation behaviour of the δ-ferrite and its effects on LCF behaviour of SS welds and weldments are required before the variation in properties between the weld metal and base metal are treated explicitly and quantitatively. In view of this, a comparative evaluation of LCF lives and cyclic stress-strain properties, deformation and fracture behaviour has been conducted on type 304 SS base, 308SS welds and 304/308 SS weldments[62] as well as 316L(N) base, 316 welds and 316L(N)/316 SS weldments[63,64]. Creep-fatigue interaction of 308, 316(N) and 316 SS welds has been explored[65-67]. Assessment of the effect of weld imperfections on LCF properties of 308 SS welds has also been made[68].

A brief discussion of the results obtained on the LCF behaviour of 304 base, 308 SS weld and 304/308 SS weld joints at 823 and 923 K and the effect of discontinuities on LCF behaviour at 823 K is included in this section. Microstructure of base metal consisted of equiaxed grains of 75 μm while weld metal was composed of long columnar grains and vermicular d-ferrite (9 ferrite number) distributed in austenite matrix. The weldments displayed coarse grained region in heat affected zone and few deformation bands giving indication of the presence of residual stresses. The cyclic stress response behaviour of the base metal, weld metal and the weld joint differed considerably (Fig. 24). Base metal showed rapid initial hardening followed by well-defined saturation stress stage. Type 308 SS weld metal exhibited continuous cyclic softening. Weldments initially hardened and then softened gradually prior to the rapid stress decrease. Weldments subjected to a stress relieving heat treatment displayed lower response stresses compared to the untreated weldments. The initial hardening observed in base metal has been attributed to the combined effects of dislocation-solute atom and dislocation-dislocation interactions, while the stress saturation has been found to have correlation with the development of well defined cell structure. The TEM studies on 316 SS weld metal provided the information on the origins of cyclic softening in austenitic weld metals[64]. The untested weld metal revealed very high density of dislocations and dislocation tangles in austenite matrix with comparatively lower density of dislocations in δ-ferrite. After LCF testing, the dislocation density in austenite was considerably reduced while δ-ferrite was free from dislocations. It was inferred that during

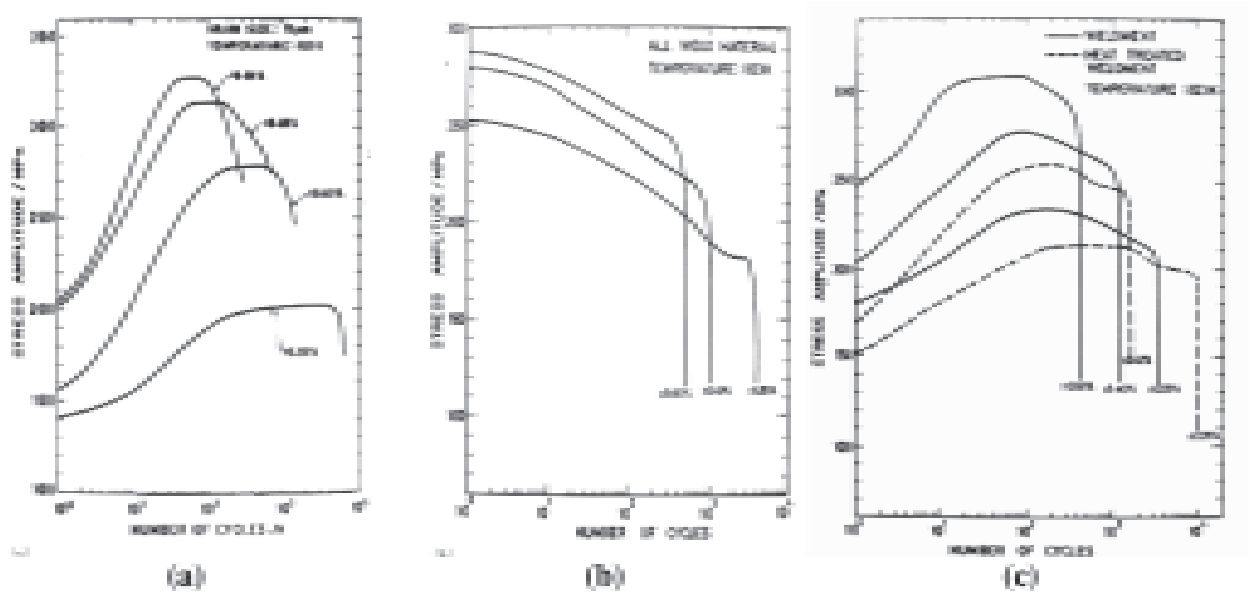

Fig. 24: Cyclic stress response curves for (a) base, (b) all weld and (c) weldments specimens at 823 K[62]

LCF, dislocation tangles break down, and subsequent annihilation of dislocations of opposite sign occurs during their to and fro motion, promoting cyclic softening. Type 304 SS base metal exhibited better LCF resistance while 304/308 SS weld joints showed the least at 823 K and 923 K (Fig. 25). Weld metal possessed lower life than base metal at 823 K and displayed slightly better life at 923 K at lower strain

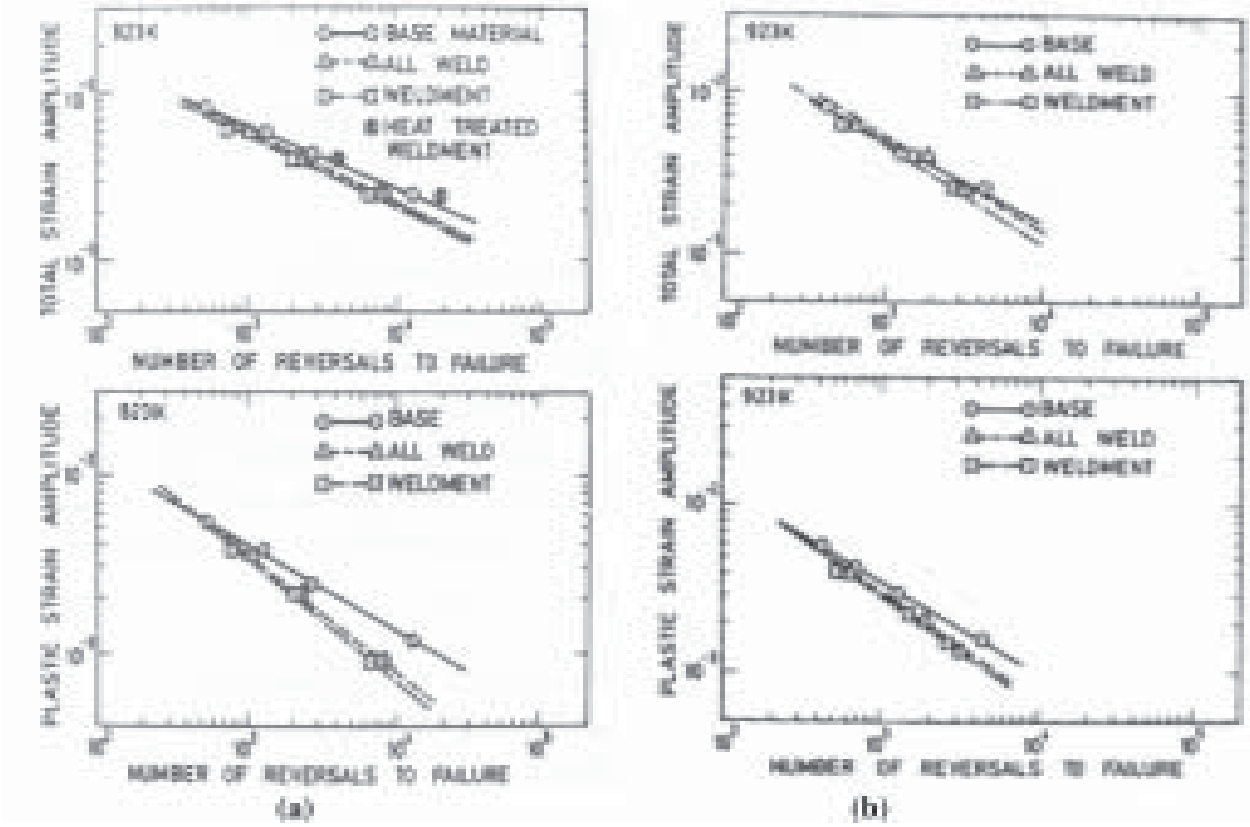

Fig. 25: Strain-life plots for base, all-weld and weldments at a) 823 K and b) 923 K[62]

amplitudes. The reduction in life was noticed for all the conditions when the temperature was raised from 823 to 923 K. The poor fatigue resistance of weldments has been ascribed to the shortening of crack initiation phase and to poor crack propagation resistance of the coarse grained region of the heat affected zone. Solution annealing (at 1173 K for 3h) the weldments prior to LCF testing caused in improvement in fatigue life probably due to the elimination of residual stresses from the weld joint. The reduction in life with increasing temperature resulted from the combined effects of an increase inelastic strain generated in a cycle and from the effects of oxidation-assisted crack initiation and propagation in all the three material conditions. Vermicular δ-ferrite in welds and weldments transformed to $M_{23}C_6$ and σ-phase during LCF testing. The transformed portion of δ-ferrite increased with increasing number of cycles to failure and increasing temperature (Fig. 26a). The transformation of δ-ferrite was more rapid in weldments than in all-weld metal. The fine duplex austenite-ferrite microstructure in the weld metal, with its transformed δ–σ phase boundaries, offered greater resistance to the extension of fatigue cracks by causing the deflection of crack path (Fig. 26b). Crack deflection could cause reduced stress intensity at the crack tip with an associated reduction in the crack propagation rate. However, at 823K, the transformation of the δ-ferrite to σ was less and the beneficial effects of crack deflection could not be seen, as a result the weld metal exhibited lower life than base metal.

Detailed investigations have been performed for assessing the significance of weld discontinuities on LCF behaviour of 308 SS welds. Weld pads were prepared by shielded metal arc welding process. Porosity and slag inclusions were introduced deliberately into the weld metal by grossly exaggerating the conditions normally causing such defects (Fig. 27a). Base metal showed higher fatigue life than sound weld metal at all strain amplitudes (Fig. 27b). The presence of porosity and slag inclusions in the weld metal led to significant reduction in life (Fig.27b). Porosity on the specimen surface has been found particularly harmful and caused a reduction in life by a factor of seven relative to sound weld metal. Defect combination of porosity and slag inclusions was found more deleterious than the case when either the slag inclusions or porosity was present alone. Discontinuities acted as crack initiation sites and also enhanced crack propagation.

7. CREEP-FATIGUE-ENVIRONMENT INTERACTIONS

7.1 Hold Time Tests on Alloy 617 at 1223 K

The effects of hold-time and strain rate on creep-fatigue-environment interactions are explained below with the aid of the tests performed on Alloy 617 at 1223 K in simulated helium gas environment of high temperature gas cooled reactor[69-71]. The helium gas was composed of 500, 20, 1.5, 15, 1 and 5 μ bar of H_2, CH_4, H_2O, CO, CO_2 and N_2 respectively.

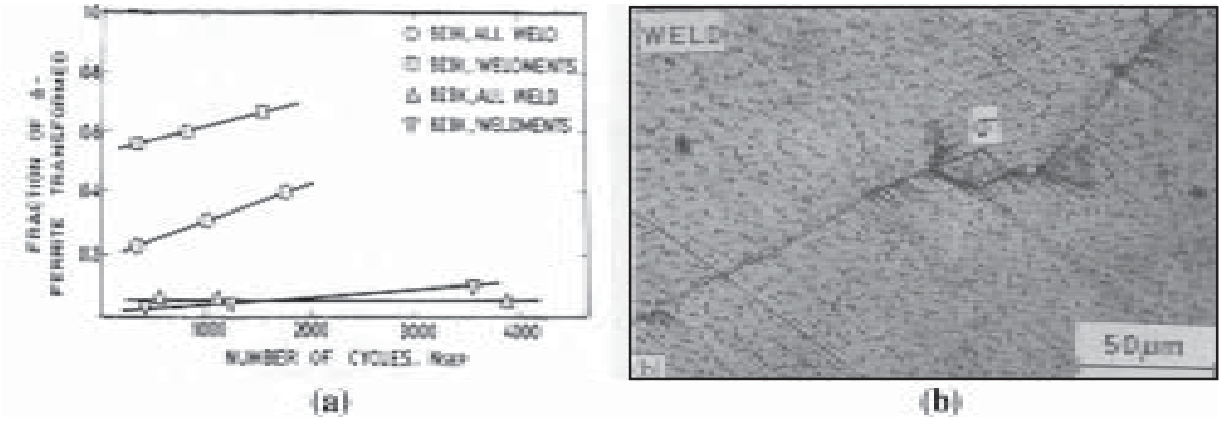

Fig. 26: (a) Influence of testing variables on the fraction of delta ferrite transformed during fatigue deformation and (b) Crack path diversion along the transformed delta ferrite regions of all-weld material at 923 K[62]

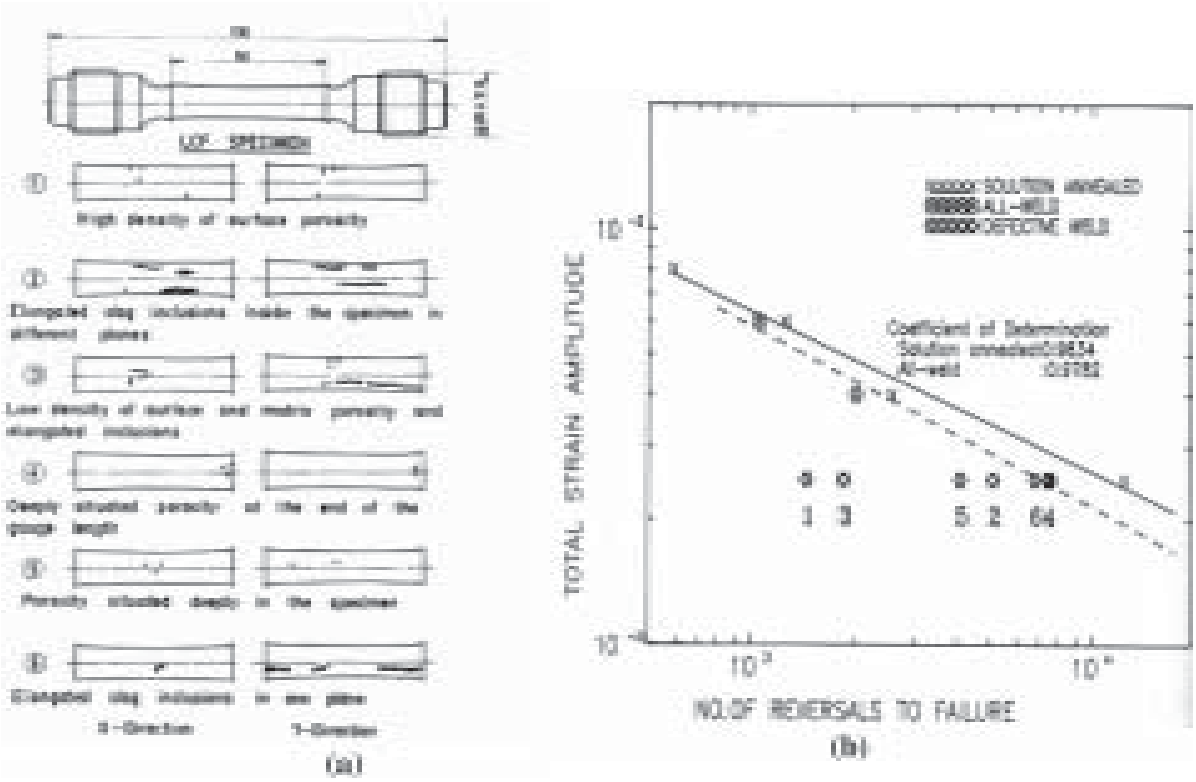

Fig. 27: a) Description and location of defects in LCF specimen of weld metal and b) Strain-life plots of 304 SS base and 308 SS sound weld and defective weld metal. Numbers at data points refer to the samples[68]

The fatigue life reduction factor (R) is defined as the ratio of life recorded for a given strain rate or hold time to the reference life value for continuous cycling at a strain rate of 4 x 10^{-3} s^{-1}. The reduction in the strain rate caused only a small reduction in fatigue life in the continuously cycled tests (Fig. 28). Irrespective of the position of hold at peak strain in a cycle, tension hold time always reduced fatigue life in comparison with continuously cycled tests of equal cycle duration; these reductions were only slightly higher than those observed for compression only hold tests and very much larger than those involving symmetrical hold periods in tension and compression. Tension plus compression holds exhibited only a small reduction in life with those compared to continuously cycled tests. In the continuously cycled tests failure was always transgranular with no indication of creep or oxidation damage observed.

The reductions in fatigue life which occurred when tensile hold periods were applied were principally due to the interaction between surface initiated fatigue crack and interior creep cavitation associated with grain boundary carbides. These cavities were formed during slow tensile stress relaxation period of the tensile holds. Figure 29 clearly illustrates the development of intergranular cavities (R type) associated with grain boundary precipitates. In addition to the bulk cavity damage, a large number of grain boundary wedge cracks were observed in the near-surface regions in the areas that were free from $M_{23}C_6$ particles particularly when the tension hold times were more than 10 min. (Fig.30a). The damage due to grain boundary oxidation was found to be considerable at longer tensile holds (Fig. 30b). Since most of the oxides are intrinsically brittle, the fatigue cracks in tests with longer hold periods initiated in oxides which are formed preferentially at surface-connected grain boundaries. The oxidation-induced surface intergranular cracks penetrated deeply into the interior and merged with independently formed intergranular wedge cracks in the near-surface regions and R-type cavities in the bulk.

Compression hold tests did not exhibit creep cavities in the specimen interior. In addition, none of these features such as a thick surface oxide layer, carbide free zones, and wedge cracking in the near-surface

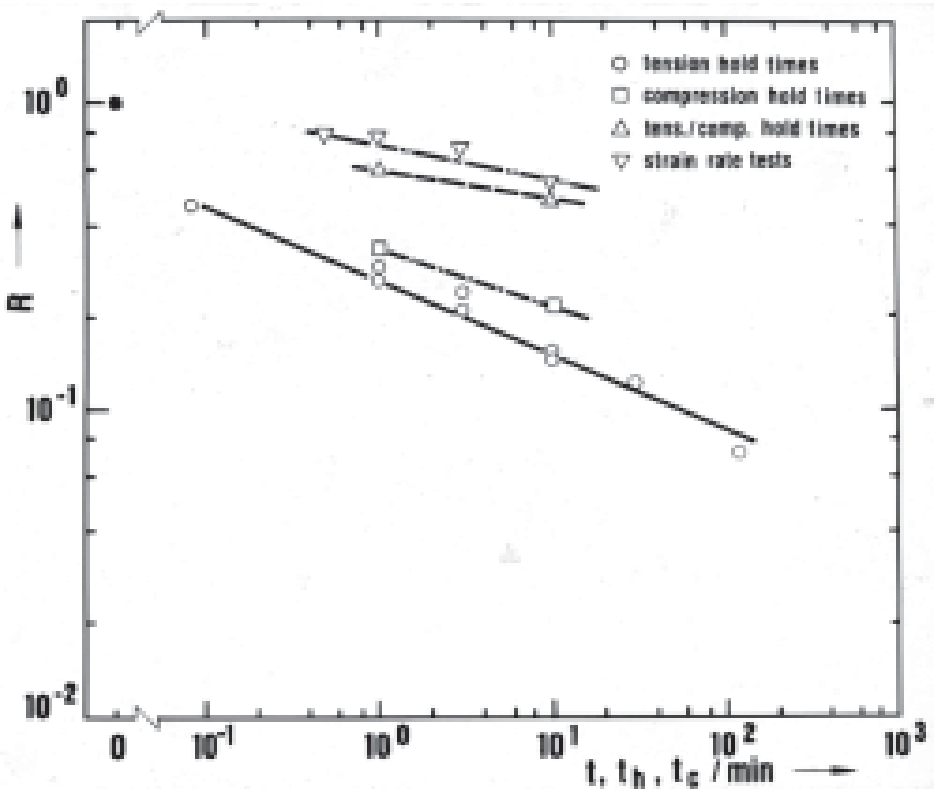

Fig. 28: The Life Reduction Factor (R) against the Cycle Period for different Loading Conditions[69]

zones which have been prominently displayed in long period tensile hold tests was found in compression hold tests. The damaging effect of compression hold was attributed to the combined effects of increased amount of inelastic strain and deformation ratcheting in the cycle. The progressive accumulation of tensile inelastic strain with continued cycling in the tensile half of the cycle and its detrimental effect compared with the accumulation of relaxation creep strain during compression holds led to tensile deformation ratcheting and tensile necking type of failure. Symmetrical holds exhibited better fatigue resistance than compression holds, in spite of higher amount of inelastic strain in a cycle and fatigue-cavity

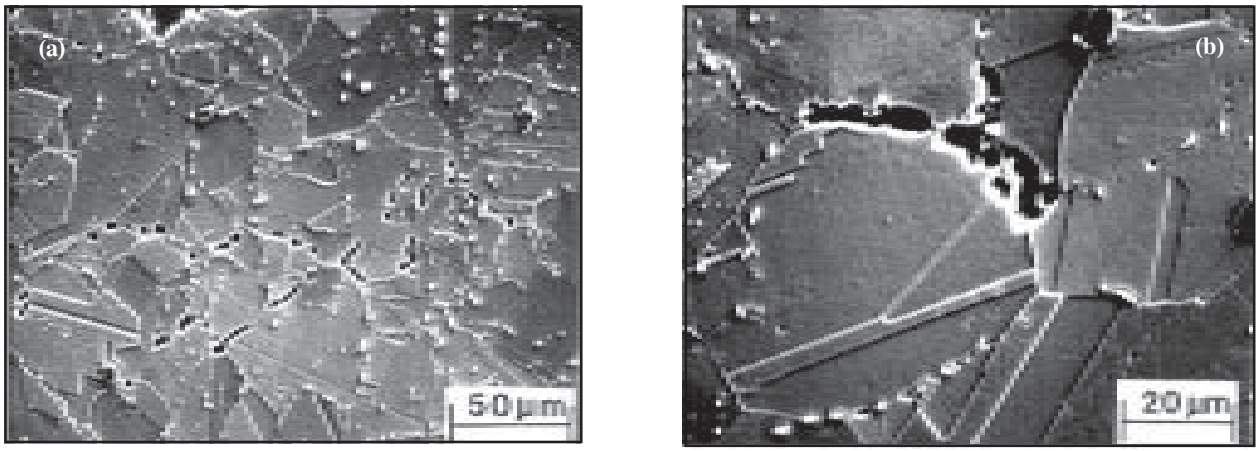

Fig. 29: (a) Creep Cavity Damage in the Interior Regions of LCF Specimen in a 1 minute Tensile Hold Test and (b) Creep Cavity Damage in the Interior Regions of LCF Specimen in a 10 minute Tensile Hold Test[69]

interactions in the vicinity of fracture zone, probably because of the non-existence of deformation ratcheting in the cycle. The cavities in the fracture zone in symmetrical holds resulted from irreversible shear deformation.

7.2 Micromechanisms Governing High Temperature Fatigue During Unequal Ramp Rate Tests in Alloy 800H

The damage mechanisms influencing the LCF behaviour of Alloy 800H at 1123 K have been evaluated under conditions of equal tension/compression ramp rates (fast-fast, slow-slow) and asymmetrical ramp rates (slow-fast, fast-slow) in tension and compression [71-73]. The effects of waveform on fatigue life of Alloy 800H is shown in Table 3.

The fatigue lives displayed by different loading conditions were in the order: F-F > S-S > F-S > S-F. The cyclic stress response was strongly dependent on waveform. The cyclic stress response was symmetrical F-F and S-S tests (Fig. 31). Asymmetrical tests displayed unequal stress amplitudes in tension and compression. The half-life hysteresis loops of F-S and S-F tests revealed large amounts of tensile and compressive mean stresses, respectively. The fracture modes depended on the tension going deformation rate. The fast deformation rate during tension going led to transgranular crack initiation and propagation

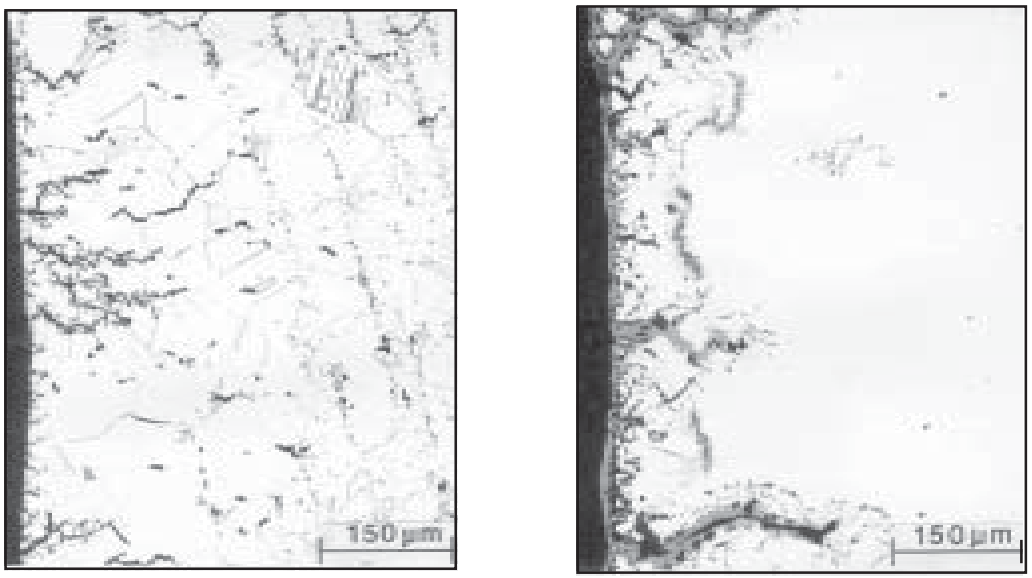

(a) (b)

Fig. 30: a) Wedge Cracking in Carbide Depleted Regions in a 10 minutes tensile hold test and (b) Oxidation in 120 min. Tensile Hold Test[69]

Table 3

INFLUENCE OF UNEQUAL RAMP RATES ON ENDURANCE OF ALLOY 800H AT 1123 K

Waveform	$\dot{\varepsilon}_t$, s^{-1}	$\dot{\varepsilon}_c$, s^{-1}	Life, cycles
F–F	4×10^{-3}	4×10^{-3}	1930
S–S	4×10^{-5}	4×10^{-5}	1180
F–S	4×10^{-3}	4×10^{-5}	990
S–F	4×10^{-5}	4×10^{-3}	380

$\dot{\varepsilon}_t$ = tension going strain rate; and $\dot{\varepsilon}_c$ = compression going strain rate.

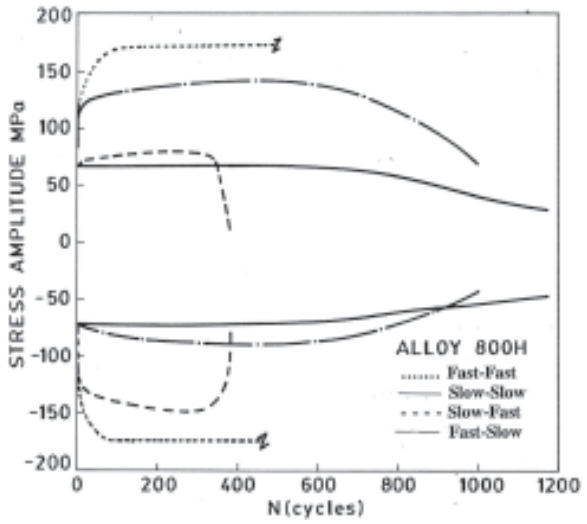

Fig. 31: Effect of Wave Shape on the Cyclic Stress Response

(Fig.32a), while slow ramping caused intergranular crack initiation and propagation. Ramping at different rates in tension and compression created deformation ratcheting in F-S and S-F tests and influenced the failure modes to a greater extent. Since deformation rates in the tension going direction are different from those in the compression going direction in F-S and S-F tests, plastic deformation in tension and creep in compression were accumulated, respectively, under F-S cycling, whereas under S-F loading creep in tension and plastic deformation in compression were accumulated, respectively. The deformation ratcheting of both plasticity in one direction and creep in another constitutes a serious damage mode in the assymetrical tests. For F-S conditions the fracture occurred by tensile necking instability (Fig. 32b). The accumulation of microscopic inelastic tensile strain, which is not recovered during the compressive portion of the cycle, would contribute to this phenomenon. The strains can become concentrated in the regions of initial plasticity, and this detrimental effect is additional to other time dependent effects. In S-F conditions, the inclusion of slow tensile strain rate into the fatigue cycle enabled creep cavitation damage to accumulate at grain boundary particles in the bulk (Fig.33a). In addition to intergranular creep damage a large number of surface intergranular cracks had initiated and grown to depths of about 1 mm (Fig. 33b). Near the surface, the environmental damage effects were severe and the diffusion of environmental species down the grain boundary can cause a reduction in the boundary cohesive strength. This effect may enhance sliding in the contaminated grain boundary and hence promote subsequent cracking. Oxidation has been found to affect primarily the initiation and near threshold crack growth stages in S-F tests. Cyclic life was influenced by synergestic interactions between a number of time-dependent mechanisms. The damage modes governing the fatigue life of Alloy 800H as a function of waveform are summarized in Table 4.

Table 4
SUMMARY OF WAVEFORM EFFECTS

Waveform	Crack Initiation and Propagation	Damage Modes
F–F	transgranular	F + MP + DSA + O
F–S	transgranular	F + O + DR + MP
S–S	intergranular	F + O + IS
S–F	intergranular	F + O + C + MP

F = fatigue; MP = massive precipitation; O = oxidation; DR = deformation ratcheting; IS = inelastic strain; and C = creep damage.

8. ACHIEVEMENT OF HIGH FATIGUE RESISTANCE IN INTERMETALLICS

There would be considerable benefit in developing new structural materials where high use temperatures and strength coupled with low density are minimum capabilities. Nickel aluminides exhibit considerable

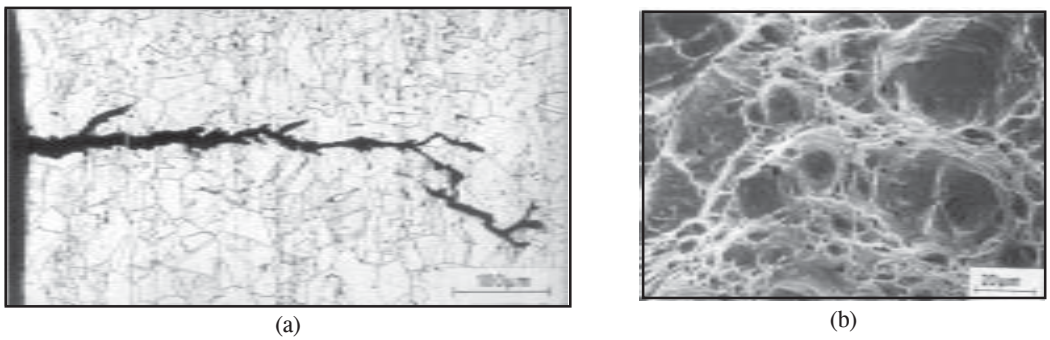

(a) (b)

Fig. 32: a)Transgranular cracking during a fast-fast test, and b) Transgranular fracture at 1123 K in a fast-slow test

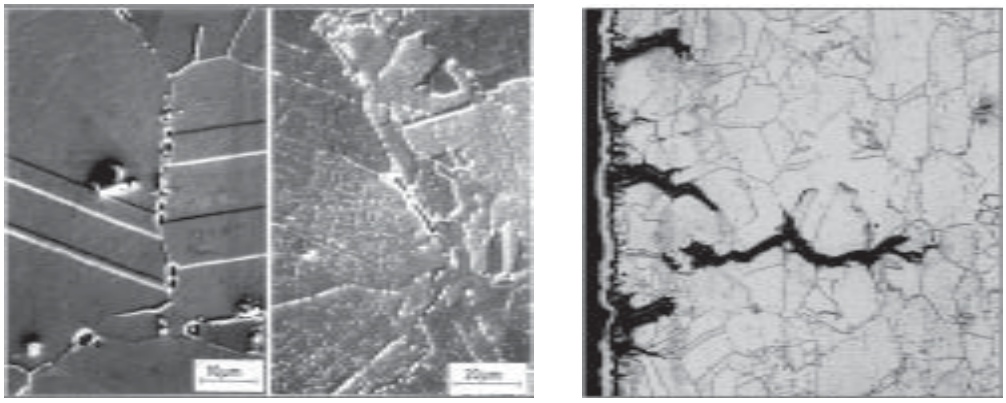

(a) (b)

Fig. 33: a) Intergranular cavitation at 1123 K and b) Intergranular crack initiation in the surface oxide scales in a slow-fast test.

potential for near-term application in various branches of modern industry due to number of property advantages including low density, high melting temperature, high thermal conductivity, and excellent environmental resistance, and the amenability for significantly improving creep and fatigue resistance through alloying. However, the B2 nickel aluminides are challenged by lack of ambient temperature ductility and toughness. These deficiencies severely impose limits on the fabrication and forming of these materials. Furthermore, binary NiAl suffers from lack of strength and poor creep resistance at and above 1000 K. Poor creep resistance in turn affects LCF lives at low strain ranges due to interaction of creep damage. Attempts have been made to improve the fatigue resistance of the NiAl by understanding the effects of manufacturing process and micro alloying.

8.1 Effects of manufacturing processes on strain controlled low cycle fatigue behaviour of polycrystalline NiAl

The NiAl samples were produced by three different processing routes: hot isostatic pressing (HP) of pre alloyed powders, extrusion of pre-alloyed powders (PE), and extrusion of vacuum induction melted ingots (CE)[74]. The HP alloy had larger grains and larger variation in grain size compared to the fully recrystallized extruded materials, CE and PE. The HP material contained prior particle boundaries that were composed of narrow stringers of fine Al_2O_3 particles. The CE material consisted of internal voids, which were aligned parallel to the extrusion axis. Despite the 12:1 reduction ratio during extrusion, the CE alloy possessed residual porosity, owing to the presence of entrapped gas. The PE alloy was fully consolidated with fewer defects than the CE or HP material.

CE and PE alloys exhibited similar lives under identical strain ranges (Fig. 34a). The HP alloy displayed shorter lives than the extruded materials, with an increasing difference in life at low strain ranges. Typically, the alloy in all processing conditions exhibited relatively little cyclic hardening or softening at 1000K. However, the HP alloy displayed a higher cyclic stress response over the entire life range compared to the extruded alloys (Fig. 34b). All the three alloys exhibited intergranular crack initiation and propagation prior to the onset of transgranular cleavage overload failure (Fig. 35). The HP alloy had much smaller zone of slow and stable intergranular crack growth compared to the extruded alloys; higher response stresses would act to reduce the critical crack size for final fracture reducing the number of cycles to failure. The relatively fast and unstable transgranular cleavage has set in much earlier in the HP alloy. In the case of HP alloy, the samples cycled at low strain ranges exhibited much shorter lives than would be expected by extrapolation from high strain range regime of the strain-life plot. The discontinuity in the strain-life curve in the HP alloy has occurred as a consequence of the operation of different damage mechanisms in the high and low life regimes. Failure of HP alloy at low strain ranges was attributed to an environmentally assisted fatigue damage mechanism that was aggravated by extensive void formation on grain boundaries owing to creep.

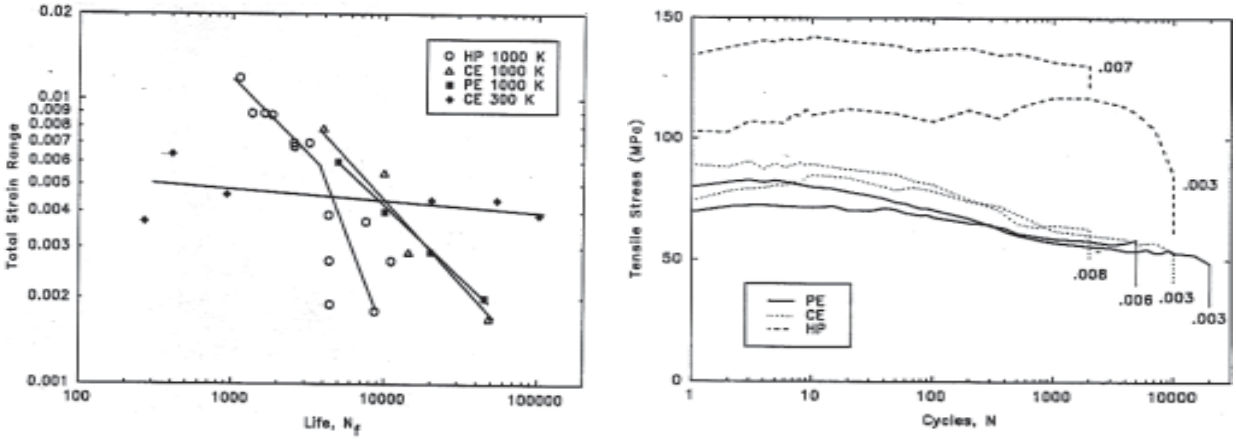

Fig. 34: a) Fatigue life curves on a total strain range basis ; b) Effect of processing on stress response of binary NiAl at 1000 K

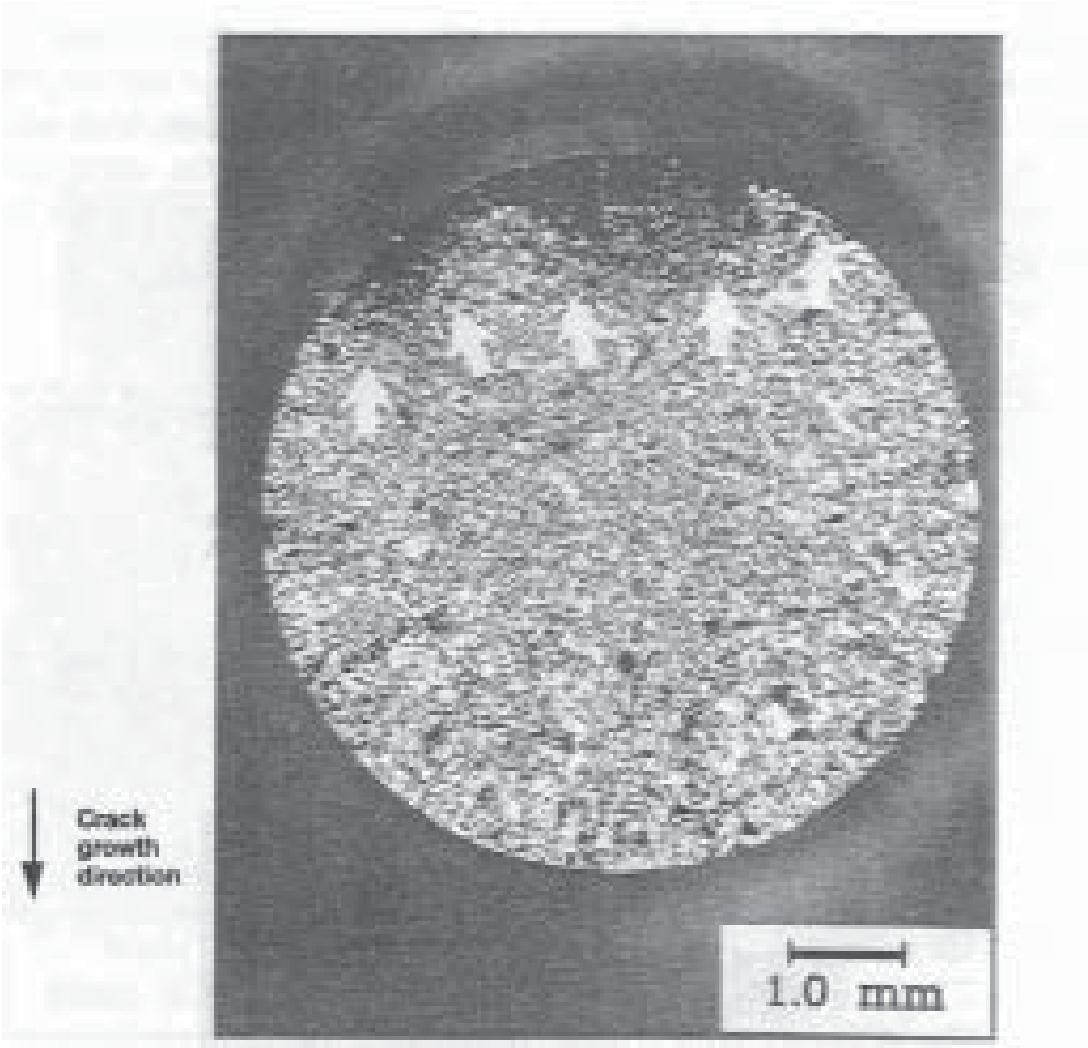

Fig. 35: Fracture surface of HP sample test at 1000 K. Arrows indicate extent of slow crack growth.

At high strain ranges, life was predominantly dictated by fatigue crack initiation and growth. The alumina particles on the grain boundaries acted as preferential sites for nucleation of creep cavities in the HP condition. These results indicate that the oxide particles in the HP samples are a major source of concern. These have significantly contributed to the large amount of scatter observed in life at low strain ranges. It has been suggested that strict control over the powder cleanliness needs to be exercised in order to improve the fatigue life in the alloys processed by HP route.

The comparative evaluation of fatigue life of NiAl and lives of various turbine disk and blade alloys at temperatures of approximately 1000 K are made in Figs. 36a and b. Binary NiAl exhibited superior fatigue life when compared to most superalloys on a plastic strain basis, but inferior to most superalloys on stress

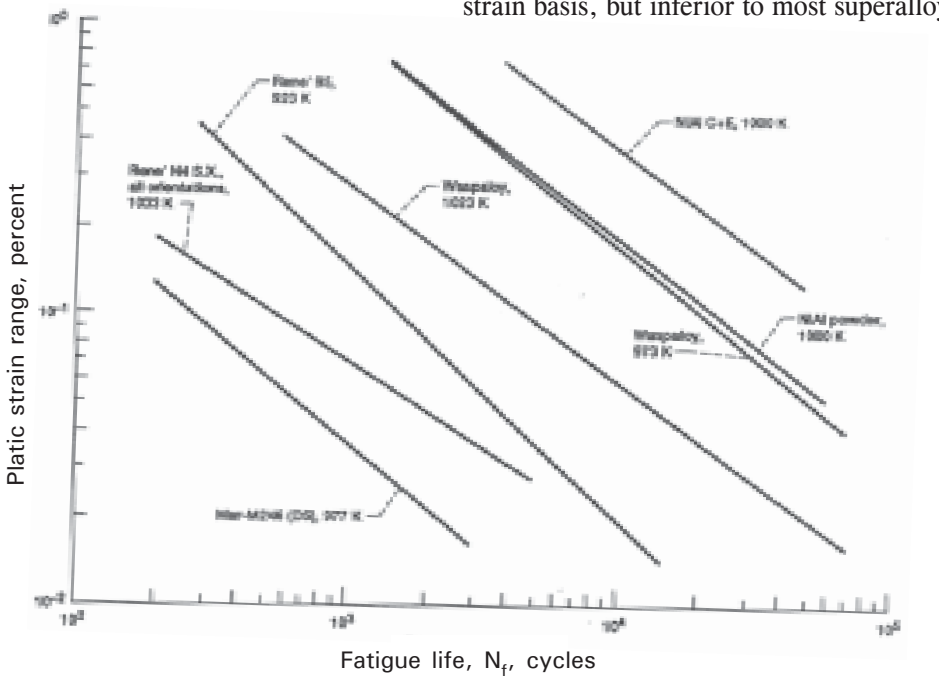

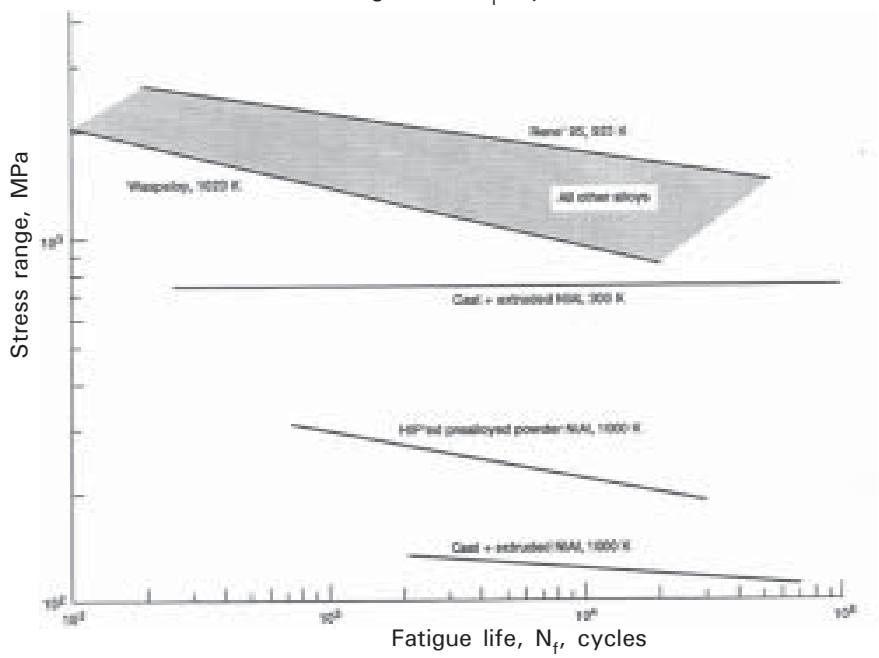

Fig. 36: (a) Fatigue life of NiAl compared to Ni base superalloys on plastic strain range basis at 1000 K.(b) Fatigue life of NiAl compared to Ni base superalloys on stress range basis at 1000 K.

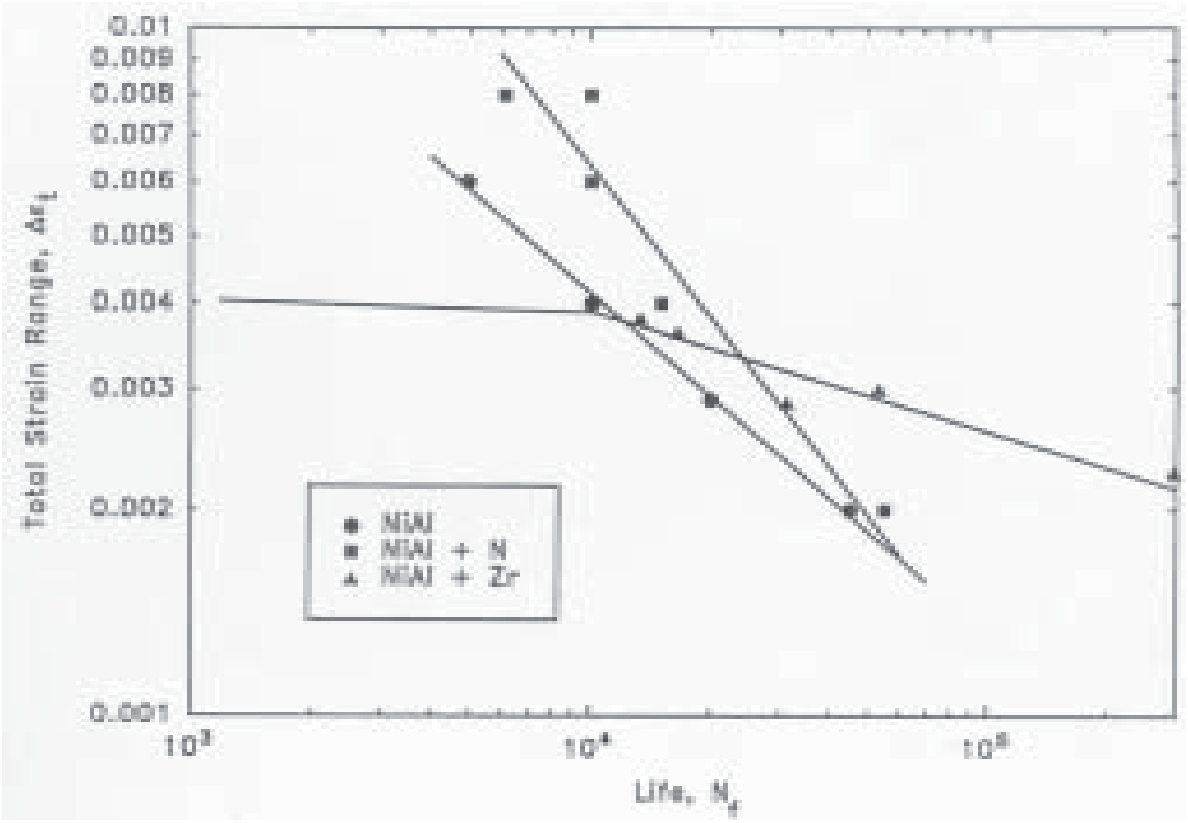

Fig. 37: Effect of processing route on strain controlled LCF behaviour of binary NiAl

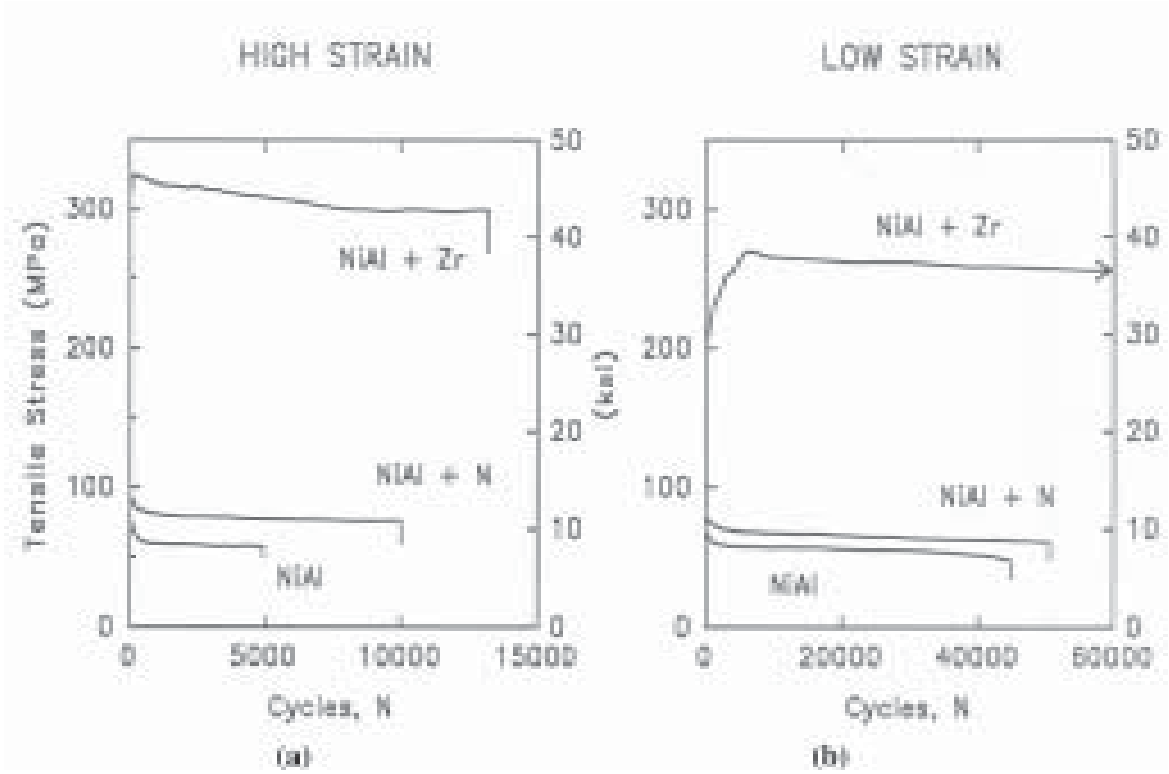

Fig. 38: Stress response curves for NiAl alloys at a) high and b) low strain ranges.

basis. The poor performance of binary NiAl on a stress range basis is due to its low yield strength compared to the superalloys. In view of this attempts have been made to improve the strength of the alloy by alloying with nitrogen as well as zirconium.

8.2 Microalloying effects on the high temperature fatigue behaviour of NiAl

The total strain fatigue resistance of NiAl (N) was higher than binary NiAl in the range of strain amplitudes examined (Fig. 37)[75-78]. Zirconium additions were even more beneficial for fatigue life at total strain ranges below 0.38%. However, on increasing the strain from 0.38% to 0.40%, the Zr-doped alloy showed a drastic reduction in life due to rapid exhaustion of its already limited ductility. There are clear differences in the stress response behaviours of binary, nitrogen-doped and Zr-doped alloys (Fig. 38). Zirconium-doped alloy displayed much higher response stresses than the other two alloys. NiAl (Zr) exhibited a short period of cyclic hardening and attained a maximum stress in the very early stages of cyclic life. Conversely, NiAl and NiAl (N) experienced cyclic softening initially followed by a period of stable stress response. Zirconium doping significantly improved cyclic strength and led to high cyclic strain hardening exponent, while the effect of nitrogen was only marginal on these properties.

The LCF behaviour of these alloys were significantly influenced by the relation between the test temperature and their respective Brittle to Ductile Transition Temperature (BDTT). Since the BDTT of NiAl (Zr) (1100 K) was higher than test temperature, substructural recovery was not significant and this led to more homogenous distribution of dislocations within the grains (Fig. 39). Additionally, Zr atoms are very effective in pinning dislocations below the BDTT and increasing the viscous drag force on dislocations at higher temperatures. Consequently, the mutual interactions between dislocations and solid solution hardening due to Zr atoms resulted in higher cyclic stress response. BDTT of the binary and N-doped alloys ($\sim$630 K) was much lower than the test temperature, significant recovery was able to occur during testing resulting in lower response stresses. The marginal improvement in cyclic stress response of the N-doped alloy over the binary NiAl has been associated with dislocation pinning by the finely dispersed AlN particles in the former alloy.

The two stages in the strain-life plot of NiAl (Zr) occurred as a consequence of the change in fracture behaviour from slow and stable intergranular crack growth at strain ranges $\leq$ 0.38% to brittle cleavage-dominated overload fracture at high strain ranges (Fig. 40). At strain ranges above 0.38%, the peak tensile stress reached the monotonic cleavage fracture

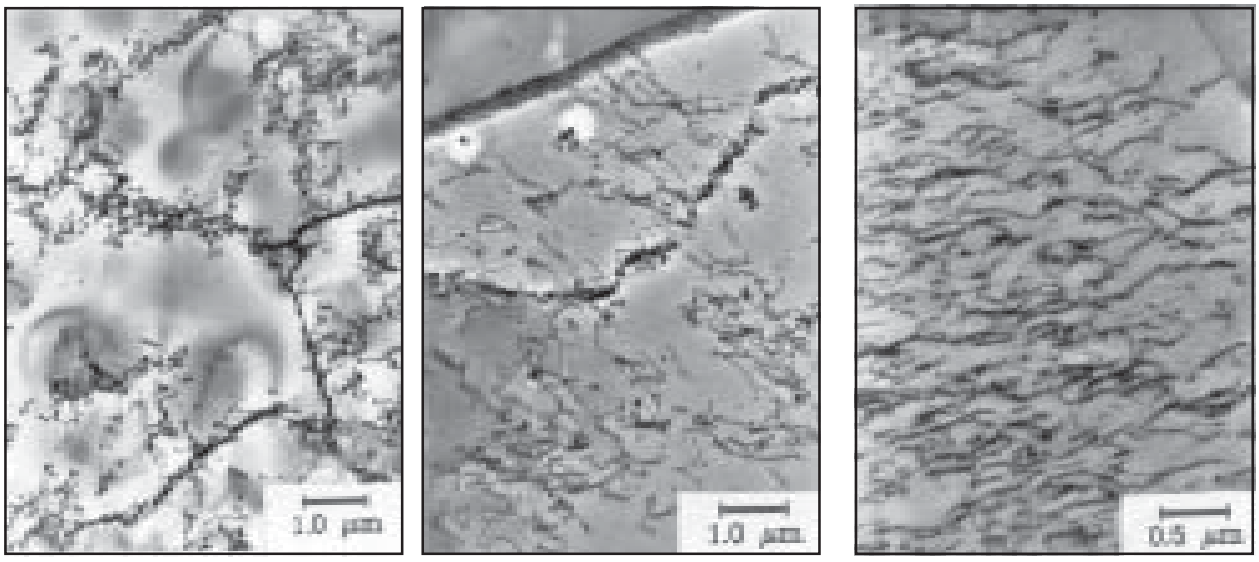

(a) (b) (c)

Fig. 39: Deformation substructures in Cyclically deformed NiAl Alloys at a total strain range of 0.3% (a) NiAl, (b) NiAl (N) and (c) NiAl(Zr)

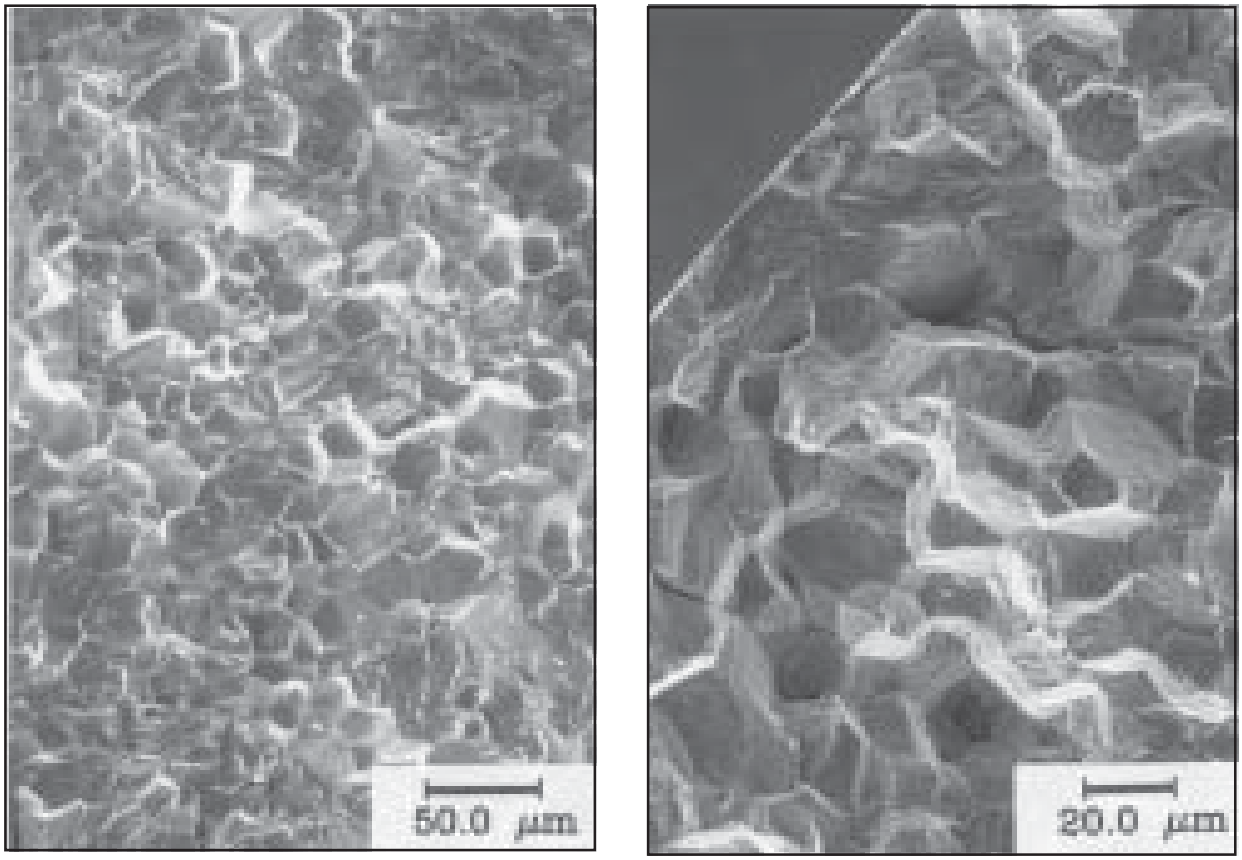

(a) (b)

Fig. 40: Fatigue damage in NiAl(Zr) (a) Mixed mode fracture with significant cleavage at a strain range of 0.40% and (b) Completely intergranular fracture at a strain range of 0.30%

stress of the Zr-doped alloy in less than 100 cycles, enabling fast crack growth by transgranular cleavage. At strain ranges less than 0.38%, the peak tensile stresses remained at much lower level than the cleavage fracture stress. In general, fatigue lives are governed by the ductility of the material at high strains and by its strength at low strains. The longer lives of NiAl (Zr) at low strain ranges result from its basic capacity to resist the applied strains on the basis of high strength. Both NiAl and NiAl (N) have shorter lives at low strain ranges due to the synergistic interaction between fatigue and creep. A higher slope of the strain range-life plot of NiAl (N) reflects this interaction. In order to improve the fatigue resistance of the N-doped alloy, the grain boundaries have to be strengthened to reduce grain boundary sliding and the associated intergranular wedge cracking that was observed in these two alloys. Since Zr segregates to the grain boundaries in NiAl and apparently strengthens the boundary regions preventing grain boundary sliding, NiAl (Zr) does not suffer from this problem. It has been found that even the extremely small Zr addition (approximately 0.1 at%) significantly improves the fatigue life on a stress range basis; approaching that of superalloys (Fig.41).

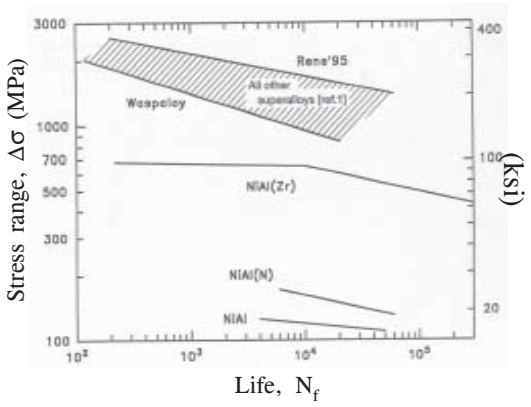

Fig. 41: Life comparison of NiAl alloys with superalloys on stress range basis at 1000 K.

9. CHALLENGES IN THE CHARACTERIZATION OF MICROSTRUCTURE AND STRAIN CONTROLLLED FATIGUE BEHAVIOUR OF A CONTINUOUS FIBER REINFORCED MMC

The development of fiber-reinforced metal matrix composites (MMC) for structural applications in airframe and aeroengine components necessitates a comprehensive understanding of strain controlled fatigue properties under fully reversed conditions. Although the thicker composites could be fabricated successfully, the characterization of strain controlled LCF behaviour remains as a challenging task since there are no guidelines whatsoever on the specimen geometry, surface finish, the method of attaching the thermocouples to the gauge section and the type of extensometry that has to be adopted. All these problems have been overcome and the suitable specimen configuration for conducting strain controlled fatigue tests has been evolved. Appropriate techniques for characterization of microstructure of fiber and composite have been developed. Comprehensive characterization led to the understanding of the starting microstructure of the composite, fatigue life of the composite in relation to the base material, cycle dependent changes in stress response and modulus of the base material and the composite, in-situ cyclic deformation of the matrix in the composite, deformation induced precipitation in the in-situ matrix and progression in the development of fatigue damage behaviour of the composite. The MMC chosen for the investigations was composed of Ti-15V-3Cr-3Al-3Sn (in wt%) matrix reinforced by continuous, unidirectional SiC(SCS-6) fibers. The 7.7 mm thick composites consisted of 32 plies of SCS-6 fibers and had a fiber volume fraction of 35%. All the fatigue specimens were heat treated prior to fatigue testing in high vacuum (10^{-6} Torr) at 973 K for 24 hours. The salient features of the starting microstructure include (i) uniform distribution of lath shaped α particles in the matrix of b.c.c .β-phase, (ii) the occurrence of TiC on some of the grain boundaries, (iii) preferential precipitation of α on some of the grain boundaries and (iv) the occurrence of precipitation lean zones next to the grain boundaries and surrounding the fibers. The microstructural features of the fiber consisted of the carbon core, the pyrolytic coating (inner), small grained SiC, large grained SiC, the carbon rich coating on the fiber outer surface, the fiber-matrix reaction zone and the matrix[80,81]. In the precipitate lean zone surrounding the fibers, matrix was deformed very heavily, and the microstructure was characterized by a very high density of planar slip bands on multiple systems (Fig. 42). The density of slip bands between the fiber rows was gradually declined as the distance from the fiber increased The effect of strain range on the evolution of cyclic tensile stress response for the unreinforced matrix and composite at 700 K (427 ^{0}C) are shown in Fig. 43. At all strain amplitudes, the composite exhibited more or less a stable cyclic stress response from the beginning[82,83]. The unreinforced Ti-15-3 alloy exhibited a stable stress response period in the initial stages followed by cyclic hardening at strain ranges below 1.5%. Cyclic stress response of the composite was higher than the matrix material at equal strain amplitudes. Fully reversed strain controlled fatigue resistance of composite is only marginally lower than that of base material (Fig. 44). Composite resisted the imposed strain elastically. Though the stress-strain hysteresis loops of the composite revealed a very limited amount of plasticity, the TEM examination of the composite foils illustrated that the in-situ matrix has accumulated substantial amount of plastic deformation during cyclic loading.

In-situ matrix deformation and precipitation behaviour was heterogeneous and varied in a complex manner. TEM microstructure of the composite in the vicinity of fiber after fatigue deformation revealed rows of secondary α laths in the β-grain (Fig. 45). It appeared that these α plates were nucleated along the slip bands that were present in the aged microstructure prior to fatigue testing. In contrast to the α plates noticed at the fibers in between the rows, the secondary α at other locations has been found to appear in the form of needles and as well as fine aggregates. Uniformly distributed fine needle-like α precipitated more predominantly in between the plies and particularly in the central locations of the matrix that was bounded by the four fibers (picture marked Q in Fig. 45b). In general, the α aggregates have occurred very predominantly in the areas close to the α lean zones found in the starting microstructure. The strain range employed in fatigue testing played a significant role

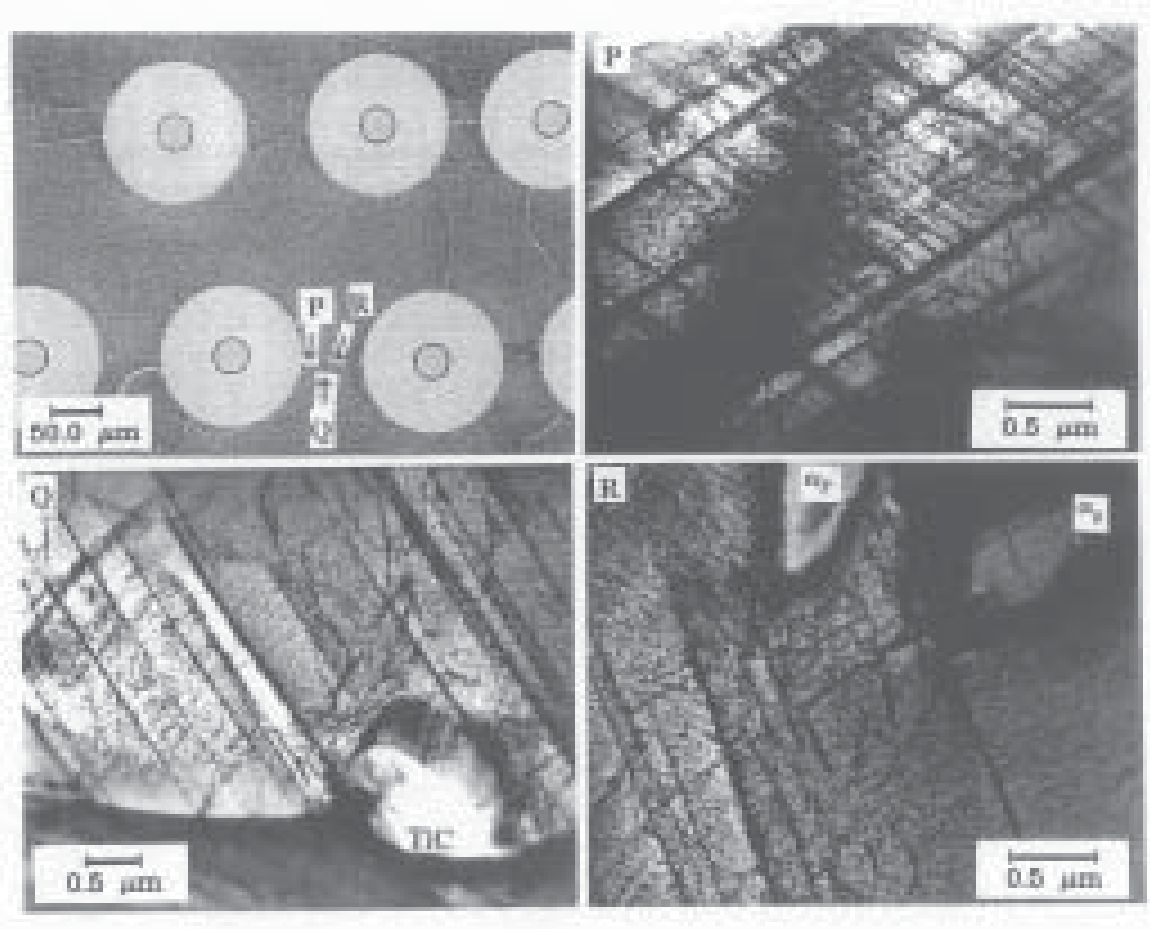

Fig. 42: Deformation substructure in the aged composite at various locations

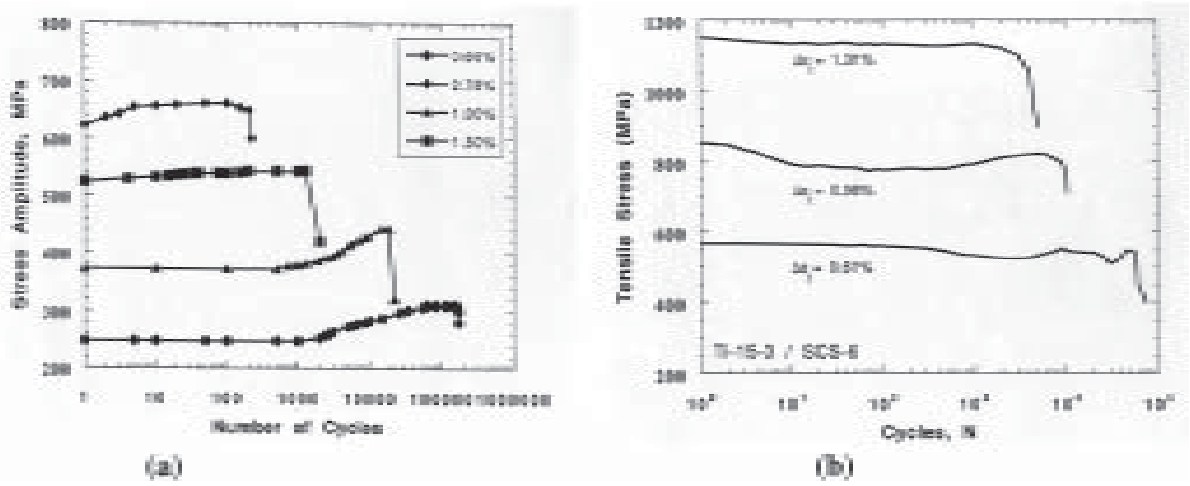

Fig. 43: Cyclic stress response curves for (a) aged Ti-15-3 matrix and (b) Composite

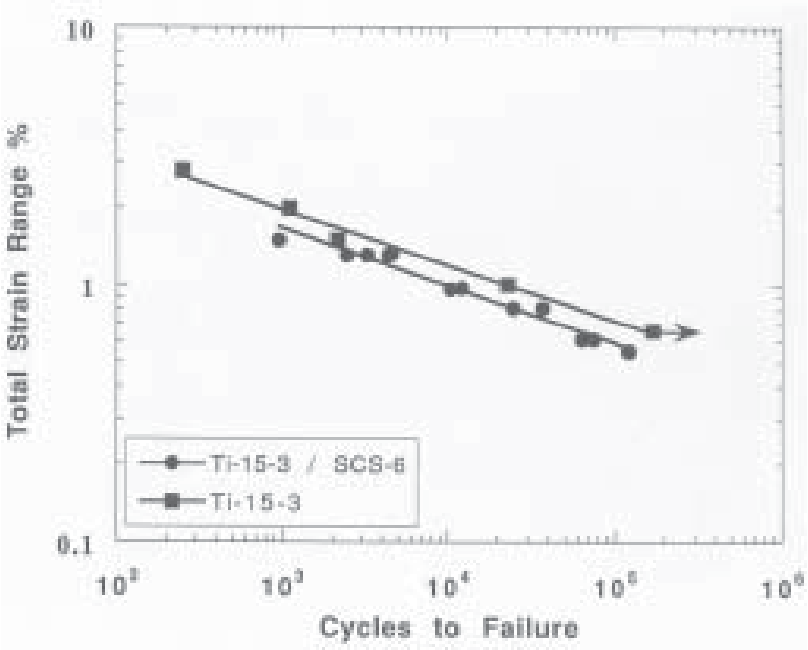

Fig. 44: Strain-Life plots for the Ti-15-3 matrix and Ti-15-3/SCS-6 composite

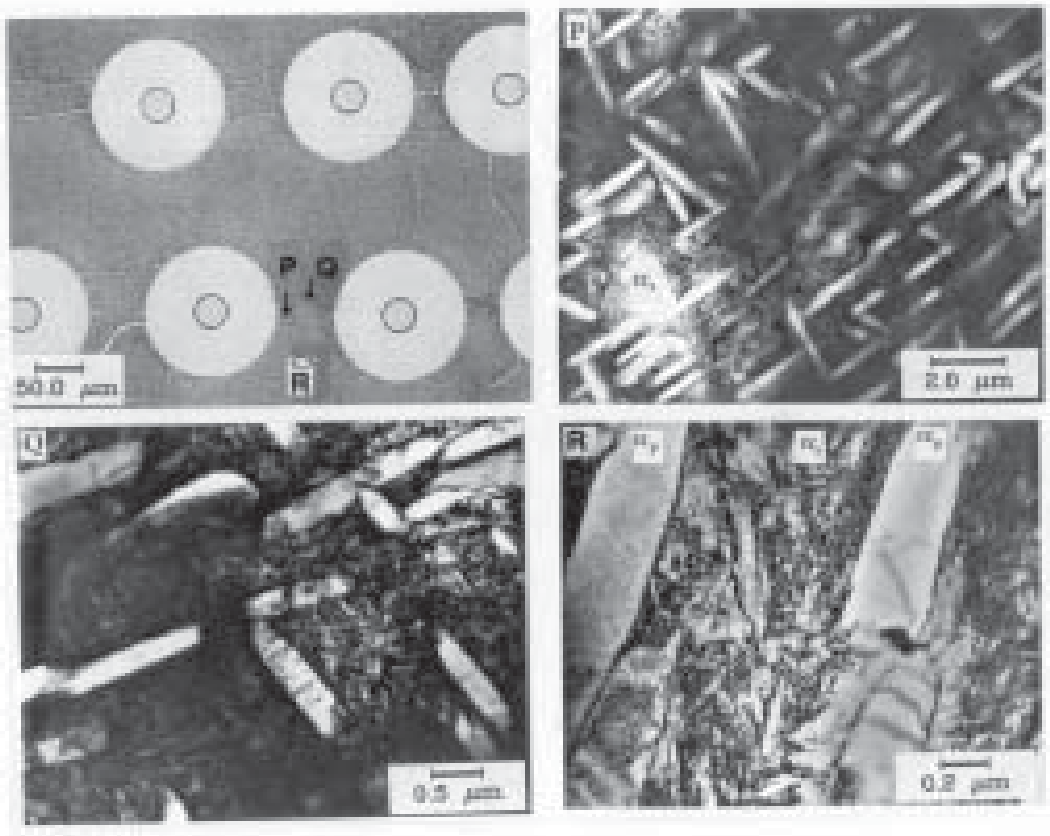

Fig. 45: (a) Precipitation of secondary α in the in-situ matrix of the composite at various locations during fatigue testing (Δε – 0.61%). All the particles in P are α_s. Large particles in Q and R are α_p.

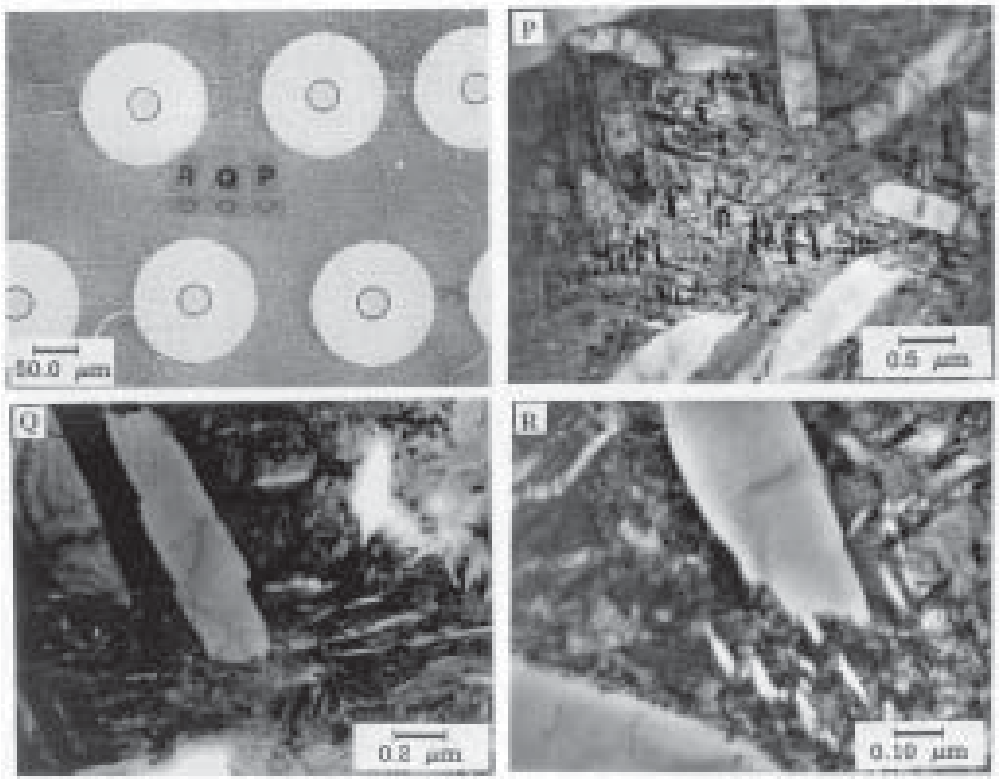

Fig. 45: (b) Microstructure of the in-situ matrix of the composite at various locations after fatigue testing ($\Delta\varepsilon$ – 0.61%)

in the precipitation behaviour. At low strain ranges, the secondary α precipitation was noticed to be significant and the size of precipitates was comparatively large.

Polished metallographic sections of the selected specimens revealed the dominance of matrix cracking at all the strain ranges; the fibers remained unbroken and bridged the cracked matrix. This observation suggests that the matrix cracked before the fiber fracture. Occasionally, fiber cracking and a few secondary cracks were observed in the matrix-fiber interfacial regions. The TEM investigations suggested that the fiber cracking could get initiated at the transition zone between the coarse grained SiC and outer carbon layer (Fig. 46), and interface between pyrolytic coating covering the carbon core and radially grown SiC layer.

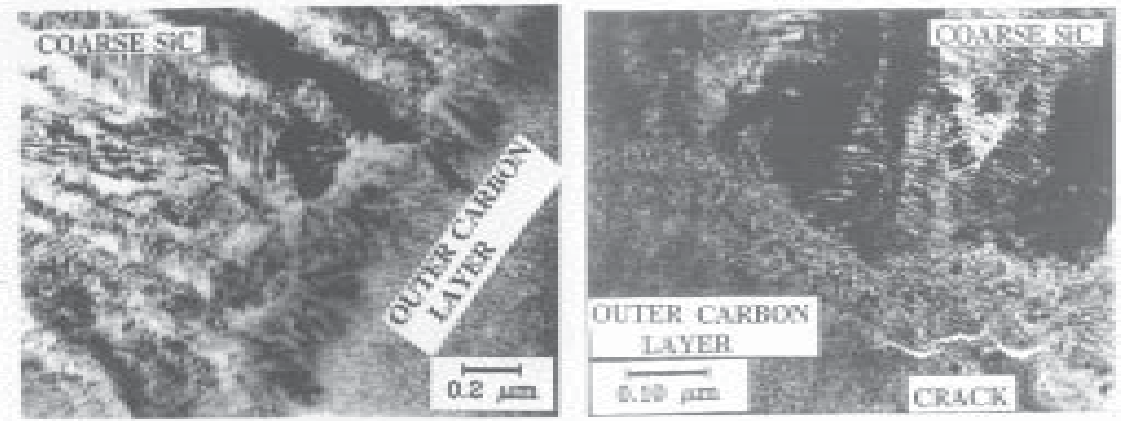

Fig. 46: Microstructure of the composite showing the coarse grained SiC, outer carbon (inner) layer and a transition zone between them (prior to fatigue testing). Fatigue cracks were noticed in this transition region of the composite ($\Delta\varepsilon$ = 1.31%).

10. CONCLUDING REMARKS

The basic understanding of high temperature fatigue in engineering materials has vastly improved over the years. There exists a number of alternative time and temperature dependent damage processes (Inelastic deformation, dynamic strain ageing, creep damage, oxidation damage, deformation ratcheting, massive precipitation, uniform matrix cavitation etc.) by which a material's life in high temperature LCF may be controlled. Each process occupies a characteristic range of temperatures, strain amplitudes, strain rates and hold times and are strongly influenced by type of material and its initial and evolving microstructure in service. The limits of their regime of dominance may be shifted and the cyclic life of the material within a particular regime of dominance may be altered by varying the cycle type, by changing the environment and as a result the occurrence of microstructural instabilities. In high temperature LCF empirical lifetime prediction methods are premised on the interaction of the fatigue deformation process with one or more of the alternative time dependent damage processes presented in this paper. The application of any lifetime prediction method is limited to the regime of dominance of the particular time dependent process. The identification of these processes and their synergistic interactions and the fixation of their limits of operation will be of assistance in materials development, selection of engineering materials for a particular application, development and selection of the most appropriate life time prediction method and with the definition of its limits of extrapolation. Because of the large number of variables in LCF, Creep-fatigue and TMF testing and the inherent problem of not being able to test for all possible combinations of variables, it is necessary to develop a mechanistic understanding of synergistic interactions in high temperature fatigue.

ACKNOWLEDGEMENTS

I have a great pleasure in placing on record my gratitude to Dr. Placid Rodriguez for introducing me to research work in mechanical metallurgy, meticulous supervision of my research work, motivating and carefully nurturing my career and providing invaluable guidance throughout his stay at Kalpakkam. I am thankful Dr. Baldev Raj, Director, IGCAR, Kalpakkam for his keen interest on my work, constant support, advice and encouragement without which this endeavour would not have been possible. He has also motivated me for conducting high quality research work with devotion and commitment to excellence. It is a pleasure to acknowledge the benefits of many illuminating discussion I had with him over the years. In my long and very fulfilling professional career, I have been fortunate to receive tremendous support, co-operation and valuable guidance from Dr. S.L. Mannan, Director, Metallurgy and Materials Group, IGCAR, Kalpakkam. The golden period of our combined research work will forever be gratefully remembered.

I am indebted to my colleagues Dr. M. Valsan and Dr. R. Sandhya for their enthusiastic participation, involvement and active co-operation in the early stages of our research work on high temperature fatigue. We have shared many of our ideas and excitements with useful discussion. The present and past members of Mechanical Metallurgy Division at Kalpakkam who have been mainly responsible for the large number of its achievements are Dr. M.D. Mathew, Dr. M. Valsan, Dr. K.G. Samuel, Dr. C. Phaniraj, Dr. G. Sasikala, Dr. B.K. Choudhary, Dr. K. Laha, Dr. R. Sandhya, Dr. V.S. Srinivasan, Mr. A. Nagesha, Mr. R. Kannan, Mrs. S. Latha, Mrs. Vani Shankar, Mrs. K.S. Chandravathi, Dr. E.Isaac Samuel, Mr. M. Nandagopal, Mr. C. Girish Sastry, Mr. Sunil Goyal and Mr. V. Ganesan. It has been a wonderful experience working with them, which will always be cherished. Dr. S. Venugopal and the entire group of INSOT facility have extended their support in the research activities of MMD. Their contributions are gratefully acknowledged. I wish to acknowledge the useful discussions that have occurred over the years with Dr. M. Vijayalakshmi, Dr. T. Jayakumar, and (Late) Dr. D. Sundararaman at IGCAR, Kalpakkam. I am gratefully indebted to Dr. G.R. Halford of NASA Glenn Research Center, Cleveland and Dr. H. Schuster and Prof. H. Nickel of Forschungszentrum, Juelich for their countless conversations about fatigue and cyclic deformation of high temperature materials. I am thankful to my research collaborators Dr. B.A. Lerch, Mr. M.G. Castelli, Dr. Sreeramesh Kalluri, Dr. R.D. Noebe at NASA Glenn Research Center. There are several people who have always evinced keen interest in my research work. They are Prof. P. Rama Rao, Prof. S. Ranganathan, Prof. P. Ramachandra Rao,

Dr. R. Krishnan, Dr. C.G.K. Nair and Dr. S. Banerjee. I express my heartful thanks to them.

I appreciate the valuable help rendered by my colleague Mr. R. Kannan in the preparation and careful reading of the manuscript.

Words are inadequate to express appreciation to my wife Mrs. Sujata, for her wisdom in life, understanding and extreme patience displayed, and for giving me full support through all these years.

REFERENCES

1. Rodriguez P and Bhanu Sankara Rao K, *Progress in Materials Science,* **37** (1993) 403

2. Bhanu Sankara Rao K, "Influence of Metallurgical Variables on the Low Cycle Fatigue Behaviour of Type 304 Stainless Steel: Grain Size, Cold Work and Thermal Ageing Effects" Ph. D Thesis, University of Madras and IGCAR Kalpakkam, India (1989).

3. Bhanu Sankara Rao K *Trans III,* **42 (Supplement)** (1989) S61

4. Bhanu Sankara Rao K, Schiffers H, Schuster H and Nickel H, *Metall. Trans.A* **19A** (1988) 359

5. Bhanu Sankara Rao K, Castelli M G, Allen G P and Ellis J P, *Metall Trans A* **28A** (1997) 347

6. Bhanu Sankara Rao K, Valsan M, Sandhya R, Mannan S L and Rodriguez P, *Trans IIM,* **44** (1991) 255

7. Bhanu Sankara Rao K, Schiffers H, Schuster H and Halford G R, *Metall Mater Trans A* **27A** (1996) 255

8. Valsan M, Sastry D H, Bhanu Sankara Rao K and Mannan S L, *Metall Mater Trans A* **25A** (1994) 159

9. Castelli M G, Miner R V and Robinson D A, *ASTM STP* **1186** (1993) 106

10. Castelli M G and Ellis J R, *ASTM STP* **1186** (1993) 195

11. Pototzky, Maier H J and Christ H J, *Metall Mater Trans A* **29A** (1998) 2995

12. Bhanu Sankara Rao K, Mannan S L and Rodriguez P, *Grain Size Effects in Strain Controlled LCF Deformation Behaviour of Type 304 Stainless Steel,* Proc. 20th RISO Intl. Symp "Materials Science: Deformation induced Microstructures – Analysis and Relation to Properties" (Eds) Bilde- Sorensenpet J P et. al. RISO National Laboratory, Roskilde, Denmark (1999) p459

13. Mannan S L and Bhanu Sankara Rao K, *Influence of Microstructure on Low Cycle Fatigue ,* Proc. Int. conf. "Recent Advances in Fracture" (Eds) Mahidhara R K et. al., TMS (1997) p213

14. Antolvich S D and Singh S B, *Metall Trans A* **2** (1971) 2135

15. Pineau A G and Pelluox, *Metall Trans A* **5** (1974) 1103

16. Ashby M F, *Phil Mag* **21** (1970) 399

17. Eylon D D and Bania P J, *Metall Trans A* **9A** (1978) 1273

18. Maiya P S and Majumdar S, *Metall Trans A* **8A** (1977) 1651

19. Bhanu Sankara Rao K, Valsan M, Sandhya R, Mannan S L and Rodriguez P, *Grain Size Dependence of Creep-Fatigue Environmental Interaction in AISI 304 Stainless Steel,* Proc. Int. Conf. "Creep" Tokyo, Japan, April 14018, 1986, ASME (1986) p77

20. Bhanu Sankara Rao K, Valsan M, Sandhya R, Mannan S L and Rodriguez P, *Metall Trans A* ***24*****A** (1993) 913

21. Bhanu Sankara Rao K, Valsan M, Sandhya R, Mannan S L and Rodriguez P, *Effect of Prior Cold Work on Low Cycle Fatigue Behaviour of AISI 304 SS,* "Fracture Control of Engineering Structures" Proc. ECF 6, Delft, Netherlands, June 15-20, (1986) p1599

22. Bhanu Sankara Rao K, Valsan M, Sandhya R, Mannan S L and Rodriguez P, *Fatigue Crack Initiation and Propagation Modes in Solution Annealed and Cold Worked AISI 304 SS at 300, 823 and 923 K,* Proc. Sixth Int. Conf. On "Fracture" December 4-10 (1984) New Delhi India

23. Srinivasan V S, Sandhya R, Valsan M, Bhanu Sankara Rao K and Mannan S L, *Int. J Fatigue* (2004) In press

24. Srinivasan V S, Sandhya R, Valsan M, Bhanu Sankara Rao K and Mannan S L, *Influence of Prior Cold Work on LCF Behaviour of 316L(N) Stainless Steel,* Proc Int Symp "Materials Ageing and Life Management" Oct 3-6, 2000, Kalpakkam, India, (Eds) Baldev Raj et. al., Allied Publishers Limited, Chennai (2000) p59

25. Sandhya R, Bhanu Sankara Rao K and Mannan S L, *Trans IIM,* **53** (2000) 273

26. Sandhya R, Bhanu Sankara Rao K, Mannan S L and Devanathan R, *Int. J Fatigue* **23** (2001) 789

27. Rodriguez P, Mannan S L and Bhanu Sankara Rao K, *Microstructural Dependence of Cyclic Deformation and Damage in Type 304 Stainless Steel,* Proc Int. Conf. "Advances in Computational Engineering Science" (Eds) Atluri S N and Yagawa G, Tech Science Press, Forsyth, Georgia (1997) p57

28. Sandhya R, Bhanu Sankara Rao K and Mannan S L, *Mater Sci Engng* (2004) In press

29. Bhanu Sankara Rao K, Vijayalakshmi M, Valsan M, Mannan S L and Rodriguez P, *Scripta Metall* **20** (1986) 989

30. Bhanu Sankara Rao K, Vijayalakshmi M, Valsan M, Mannan S L and Rodriguez P, *High Temp Mater Processes* **9** (1988) 1

31. Bhanu Sankara Rao K, Vijayalakshmi M, Valsan M, Mannan S L and Rodriguez P, *Scripta Metall* **23** (1989) 157

32. Bhanu Sankara Rao K, Vijayalakshmi M, Valsan M, Mannan S L and Rodriguez P, *Microstructure, Strain Amplitude and Frequency Dependence of Uniform Matrix Cavitation in Strain Controlled Fatigue,* Proc Tenth RISO Int Symp " Metallurgy and Materials Science: Materials Architecture" (Eds) Bilde-Sorensen J B et. al . RISO National Laboratory, Roskilde, Denmark (1989) p 535

33. Valsan M, Bhanu Sankara Rao K and Mannan S L *Trans IIM* **42 (Supplement)** (1989) s203

34. Valsan M, Bhanu Sankara Rao K, Vijayalakshmi M, Mannan S L and Sastry D H, *Metall Trans* **23A** (1992) 1751

35. Valsan M, Bhanu Sankara Rao K and Mannan S L, *Low Cycle Fatigue Behaviour of Nimonic PE-16 Superalloy,* Proc. 7th Int. Cont. on Fracture "Advances in Fracture Research" (Eds) Salama et. Al., Pergamon Press (1989) Vol. 2 p1323

36. Bhanu Sankara Rao K, Seetharaman V, Mannan S L and Rodriguez P, *Mater Sci Engng* **58** (1983) 93

37. Bhanu Sankara Rao K, Seetharaman V, Mannan S L and Rodriguez P, *Mater Sci Engng* **63** (1984) 35

38. Bhanu Sankara Rao K, Seetharaman V, Mannan S L and Rodriguez P, *J Nucl Mater* **102** (1981) 7

39. Kalluri S, Bhanu Sankara Rao K, Halford G R and McGaw M A, *Deformation and Damage Mechanisms in Inconel 718 Superalloy,* Proc.Superalloys 718, 625, 706 and Various Derivatives, (Eds) Loria E A, TMS (1994) p593

40. Kalluri S, Bhanu Sankara Rao K, Halford G R and McGaw M A, *Deformation Mechanisms and Fatigue Behaviour of Pre-strained Inconel 718 Superalloy,* Proc. Superalloys 718, 625, 706 and Various Derivatives, (Eds) Loria E A, TMS (1997) p595

41. Bhanu Sankara Rao K, Valsan M, Sandhya R, Mannan S L and Rodriguez P, *Metals, Materials and Processes* **2** (1990) 17

42. Bhanu Sankara Rao K, Valsan M, Sandhya R, Mannan S L and Rodriguez P, *Grain Size Dependence of DSA during LCF in Type 304 SS,* Intl.Conf. "Fracture" (Eds) Salama et. al. Pergamon Press Vol. 2 (1989) p1037

43. Bhanu Sankara Rao K, Valsan M, Sandhya R, Mannan S L and Rodriguez P, *High Temp Materials and Processes,* **7** (1986) 171

44. Sandhya R, Bhanu Sankara Rao K, Mannan S L and Devanathan R, *Scripta Metall Mater* **41** (1999) 921

45. Sandhya R, Bhanu Sankara Rao K and Mannan S L, *Mater Sci Tech* (2005) In press

46. Kannan R, Valsan M, Samuel K G, Bhanu Sankara Rao K and Mannan S L, *Trans IIM* **55** (2002) 355

47. Srinivasan V S, Sandhya R, Bhanu Sankara Rao K, Mannan S L and Raghavan K S, *Int J Fatigue* **13** (1991) 471

48. Srinivasan V S, Valsan M, Bhanu Sankara Rao K, Mannan S L and Sastry D H, *Trans IIM* **49** (1996) 489

49. Srinivasan V S, Sandhya R, Valsan M, Bhanu Sankara Rao K, Mannan S L and Sastry D H, *Scripta Materialia* **37** (1997) 1593

50. Srinivasan V S, Sandhya R, Valsan M, Bhanu Sankara Rao K, Mannan S L and Sastry D H, *Int J Fatigue* **21** (1999) 11

51. Bhanu Sankara Rao K, Castelli MG and Ellis J R, *Scripta Metallurgica et Materialia* **33** (1995) 1005

52. Bhanu Sankara Rao K, Kalluri S, Halford G R and McGaw M A, *Scripta Metallurgica et Materialia* **32** (1995) 493

53. Nagesha A, Valsan M, Bhanu Sankara Rao K, Kannan R and Mannan S L, *Trans IIM* **58** (2005) In press

54. Bhanu Sankara Rao K, Castelli M G, Allen G P and Ellis J R, *Temperature Dependent Cyclic Deformation in Haynes 188 Superalloy,* NASA-TM 107016 (1995)

55. Castelli M G, Bhanu Sankara Rao K and Ellis J R, *Micromechanisms Influencing High Temperature Fatigue Deformation in Haynes 188 Superalloy*, Proc Symp "Micromechanisms of Advanced Materials" Cleveland, November 1995 (Eds) Chu S N G et. al., TMS (1995) p197

56. Castelli M G and Bhanu Sankara Rao K, *Cyclic Deformation of Haynes 188 Superalloy Under Isothermal and Thermomechanical Loading,* Proc "Superalloys" 1996 (Eds) Kissenger R D et. al., TMS (1996) p375

57. Bhanu Sankara Rao K, *Isothermal andd Thermomechanical Fatigue Deformation of a Dynamic Strain Ageing Cobalt Base Superalloy,* Proc Int Conf

"Materials Ageing and Life Management, ISOMALM 2000" October 3-6, 2000, (Eds) Baldev Raj et. al., Allied Publishers, Chennai, Vol.1 (2000) p43

58. Castelli M G, Bhanu Sankara Rao K and Ellis J R, NASA- High Temperature Reviews, Vol. 1 (1995) 1

59. Choudhary B K, Bhanu Sankara Rao K and Mannan S L, *Mater Sci Engng* **A148** (1991) 267

60. Choudhary B K, Bhanu Sankara Rao K, Mannan S L and Kashyap B P, *Int J Fatigue* **4** (1992) 219

61. Bhanu Sankara Rao K, Choudhary B K and Mannan S L, *Metals Materials and Processes,* **4** (1992) 203

62. Bhanu Sankara Rao K, Valsan M and Mannan S L, *Mater Sci Engng* **A130** (1990) 67

63. Valsan M, Bhanu Sankara Rao K, Sandhya R and Mannan S L, *Mater Sci Engng* **A149** (1992) L9

64. Valsan M, Sundararaman D, Bhanu Sankara Rao K and Mannan S L, *Metall Mater Trans* **26A** (1995) 1207

65. Bhanu Sankara Rao K, Sandhya R and Mannan S L, *Int J Fatigue* **15** (1993) 221

66. Srinivasan V S, Valsan M, Bhanu Sankara Rao K, Mannan S L and Baldev Raj, *Int J Fatigue* **25** (2003) 1327

67. Valsan M, Nagesha A, Bhanu Sankara Rao K, Sandhya R, Mannan S L and Baldev Raj, *Trans IIM* **58** (2005) In press

68. Bhanu Sankara Rao K, Valsan M, Sandhya R, Mannan S L and Rodriguez P, *Trans ASME, J Engng Mater Tech* **116** (1994) 93

69. Bhanu Sankara Rao K, Muerer H P and Schuster H, *Mater Sci Engng* **A104** (1988) 37

70. Muerer H P, Schuster H and Bhanu Sankara Rao K, Proc Symp on "Strength and Deformation at High Temperature" Bad Naauheim FRG, April 13-14 (1989) p1

71. Bhanu Sankara Rao K, Mannan S L, Rodriguez P, Schuster H, Schiffers H, Muerer H P and Nickel H, *Low Cycle Fatigue and Creep-Fatigue-Environment Interaction,* Indo German Seminar on "Trends and Techniques in Modern Materials Research" IGCAR, Research Reort No. 99C (1988) p81

72. Bhanu Sankara Rao K, Schuster H and Halford G R, *Metall Mater Trans* **27A** (1996) 851

73. Bhanu Sankara Rao K, Schuster H and Halford G R, *Scripta Met Mater* **31** (1994) 381

74. Bhanu Sankara Rao K, Lerch B A and Noebe R D, *Effects of Processing Route on Strain Controlled Low Cycle Fatigue Behaviour of Polycrystalline NiAl,* in "Fatigue and Fracture of Ordered Intermetallic Materials II" (Eds) Srivatsan T S, Soboyejo W and Ritche R O, TMS- Warrandale (1994) p245

75. Noebe R D, Lerch B AA and Bhanu Sankara Rao K, *Assessment of Microalloying Effects on High Temperature Fatigue Behaviour of NiAl,* in "High Temperature Ordered Intermetallic Alloys VI" Proc. Materials Research Society, Vol. 364 (1995) p291

76. Bhanu Sankara Rao K, Lerch B A and Noebe R D, in "High Temperature Review-1994, NASA CP-10146 (1994) p53-1

77. Lerch B A, Noebe R D and Bhanu Sankara Rao K, *J Mater Engng Performance* **7** (1998) 205

78. Bhanu Sankara Rao K, *Sadhanna* **28** (2003) 695

79. Lerch B A, Gabb T P and Mackay R A, *Heat Treatment study of the SiC/Ti-15-3 Composite System*, NASA-Lewis Research Center, Cleveland, Ohio, NASA TP 2970 (1990).

80. Lerch BA, Hull D R, and Leonhardt T A, *As Received Microstructure of a SiC.Ti-15-3 Composite*, NASA TM 100938 (1988).

81. Lerch BA, Hull D R, and Leonhardt T A, *Composite*, **21** (1990) 216.

82. Lerch BA, Bhanu Sankara Rao K and Halford G R, Proc. Int. Conf. on "Composite Engineering, ICEE/1" New Orleans, August 1994, David Hui (Ed) (1994) p421.

83. Bhanu Sankara Rao K, Lerch B A, and Baldev Raj, *Challenges in the Characterization of Microstructure and Strain Controlled Fatigue Behaviour of Continuous Fiber Reinforced Metal Matrix Composite,* Proc. Int. Conf. "Advances in Composite" Bangalore, August 2000 (Eds) Dwarakadasa E S and Nair C G K, Vol. II (2000) p 605.